THE NATIONAL CARBON CAPTURE CENTER AT THE POWER SYSTEMS DEVELOPMENT FACILITY

TOPICAL REPORT

BUDGET PERIOD TWO
DECEMBER 1, 2009 – DECEMBER 31, 2010

DOE Cooperative Agreement

DE-NT0000749

Prepared by:
Southern Company Services, Inc.
Power Systems Development Facility
P.O. Box 1069
Wilsonville, AL 35186
Phone: 205-670-5840
Fax: 205-670-5843
http://www.NationalCarbonCaptureCenter.com

DISCLAIMER

ABSTRACT

The Power Systems Development Facility (PSDF) is a state-of-the-art test center sponsored by the U.S. Department of Energy and dedicated to the advancement of clean coal technology. In addition to the development of advanced coal gasification processes, the PSDF features the National Carbon Capture Center (NCCC) to study CO_2 capture from coal-derived syngas and flue gas.

The NCCC includes multiple, adaptable test skids that allow technology development of CO_2 capture concepts using coal-derived syngas and flue gas in industrial settings. Because of the ability to operate under a wide range of flow rates and process conditions, research at the NCCC can effectively evaluate technologies at various levels of maturity.

During the Budget Period Two reporting period, efforts at the PSDF/NCCC focused on new technology assessment and test planning; designing and constructing post-combustion CO_2 capture facilities; testing of pre-combustion CO_2 capture and related processes; and operating the gasification process to develop gasification related technologies and for syngas generation to test syngas conditioning technologies.

ACKNOWLEDGEMENT

The authors wish to acknowledge the contributions and support provided by various project managers, including Morgan “Mike” Mosser of the Department of Energy and John Wheeldon of the Electric Power Research Institute. The project is sponsored by the U.S. Department of Energy National Energy Technology Laboratory under cooperative agreement DE-NT0000749.

TABLE OF CONTENTS

LIST OF FIGURES

Figure ..... Page

LIST OF TABLES

GLOSSARY OF ABBREVIATIONS AND ENGINEERING UNITS

Abbreviations

ABC—Ammonium Bicarbonate
ASU—Air Separation Unit
B&W—Babcock & Wilcox
BOP—Balance of Plant
BP1—Budget Period One
BP2—Budget Period Two
CH_4—Methane
CO—Carbon Monoxide
CO_2—Carbon Dioxide
CPU—CO_2 Purification and Compression Unit
DCS—Distributed Control System
DEPG—Dimethyl Ether of Polyethylene Glycol
DOE—Department of Energy
EPA—Environmental Protection Agency
EPRI—Electric Power Research Institute
FEAL—Iron Aluminide
FGD—Flue Gas Desulfurization
FRP—Fiberglass Reinforced Plastic
FTIR—Fourier Transform Infrared
GC—Gas Chromatograph
H_2—Hydrogen
H_2S—Hydrogen Sulfide
HCl—Hydrochloric acid
HHV—Higher Heating Value
HMI—Human Machine Interface
ICP-MS—Inductively Coupled Plasma-Mass Spectrometer
ID—Induced Draft
IGCC—Integrated Gasification Combined Cycle
KF—Potassium Flouride
KOH—Potassium Hydroxide
L/G—Liquid-to-Gas Ratio
LCOE—Levelized Cost of Electricity
MCC—Motor Control Center
MEA—Monoethanolamine
MMD—Mass Median Diameter
MPT—Media & Process Technology
MTR—Membrane Technology & Research
$2NH_4HCO_3$—Ammonium Carbonate
$(NH_3)_2CO_3$—Ammonium Carbamate
NCCC—National Carbon Capture Center
NDIR—Non-Dispersive Infrared
NH_3—Ammonia
NMR—Nuclear Magnetic Resonance
NOx—Nitrogen Oxides
O&M—Operations and Maintenance
PC—Pulverized Coal
PC4—Post-Combustion Carbon Capture Center
PCC—Post-Combustion Capture
PCD—Particulate Control Device
PDAC—Pressure Decoupled Advanced Coal
PDMS—Polydimethylsiloxane
PLC—Programmable Logic Controller
PRB—Powder River Basin
PSDF—Power Systems Development Facility
PSTU—Pilot Solvent Test Unit
R01 through R05—Test Runs 1 through 5
R&D—Research and Development
S/L—Steam-to-Liquid Ratio
SCR—Selective Catalytic Reduction
SCS—Southern Company Services
SCU—Syngas Conditioning Unit
SEM—Scanning Electron Microscope
SO_2—Sulfur Dioxide
SOx—Sulfur Oxides
SRI—Southern Research Institute
TCA—Total CO_2 Analysis
TROC—Transport Oxy-Combustion
TSP—Technology Screening Process
WGS—Water-Gas Shift

Engineering Units

Btu—British thermal units
^{o}C—degrees Celcius
cm^2—square centimeters
cm^3—cubic centimeters
cmHg—centimeters of mercury
^{o}F—degrees Fahrenheit
ft/s—feet per second
g/cm^3—grams per cubic centimeter
g-mol—gram-mole
gpu—gas permeation unit
hr—hours
kcal--kilocalorie
k lb—kilo pound
KVA—kilovolt amps
kW—kilowatts
kWhr—kilowatt hours
kW-yr—kilowatt years
lb—pounds
lb-mol—pound-mole
lb/hr—pounds per hour
m^2—square meters
m^3—cubic meters
MM—million
mol%—mole percent
MW—megawatts
ppmv—parts per million by volume
psi—pounds per square inch
psia—pounds per square inch absolute
rpm—revolution per minute
s or sec—seconds
vol%—volume percent
wt%—weight percent

1.0 EXECUTIVE SUMMARY

The Power Systems Development Facility (PSDF) is a key national asset for ensuring continued, cost-effective, environmentally acceptable energy production from coal. Sponsored by the U.S. Department of Energy (DOE), the PSDF is an engineering scale test center located in Wilsonville, Alabama. The PSDF staff has effectively developed advanced power systems to meet the national need for cleaner, more efficient power production from coal. Building on its previous success, PSDF now houses the National Carbon Capture Center (NCCC), established in 2009 to address the nation's need for cost-effective, commercially viable CO_2 capture options for flue gas from pulverized coal power plants and syngas from coal gasification power plants.

The NCCC is leading the way to lower-cost CO_2 capture technologies and to enable coal-based power generation to remain a key contributor to providing affordable, reliable, and clean power generation. The facilities accommodate a range of equipment sizes and provide commercially representative test conditions that allow results to be scaled confidently to commercial application, a crucial element in shortening development times.

Project Partnership with DOE. The DOE conceived the PSDF as the premier advanced coal power generation research and development (R&D) facility of the world, to "serve as the proving ground for many new advanced power systems." Since operations began in 1996, the PSDF has been a center for national efforts to develop high efficiency, coal-based power generation technologies that are reliable, environmentally acceptable and cost effective. Two significant achievements–in addition to many secondary goals that were met–were the development of hot gas filtration to improve energy efficiency and the development of a gasifier suitable for use with low-rank coals. These two technologies have progressed to commercialization with integrated gasification combined cycle (IGCC) power plants under construction in Kemper County, Mississippi, and Dong Guan, China.

Project Mission and Approach. The mission of the NCCC/PSDF is to develop advanced power generation technologies to allow the continued use of coal in an efficient and environmentally clean manner, thereby supporting national, economic, and energy security. The work to be undertaken will support the next stages of coal-fired power technologies and the continued operation of conventional coal-fired power plants under CO_2 emission constraints.

In undertaking its mission, the NCCC/PSDF is involved in a range of activities to develop the most promising technologies for future commercial deployment, thereby maximizing the impact of project funds. The test facilities, shown in Figure 1, include the original PSDF site, which houses the gasification process and pre-combustion CO_2 capture test site, and the Post-Combustion Carbon Capture Center (PC4), located at a major power plant on the same Alabama Power (Southern Company) property.

Figure 1. NCCC/PSDF Facilities.

Pre-combustion CO_2 capture is vital for the advancement of efficient gasification processes needed for state-of-the-art coal-fired power plants. The backbone of the NCCC/PSDF pre-combustion CO_2 capture technology development is a high-pressure, flexible facility designed to test an array of solvents, contactors, membranes, sorbents, and water-gas shift processes. Slipstreams are available with a range of gas flow rates and process conditions using coal-derived syngas for verification and scale-up of fundamental R&D CO_2 capture projects.

The NCCC/PSDF is also exploring post-combustion capture technology development. For both new and existing power plants, post-combustion CO_2 capture must be made more efficient and cost-effective by developing alternative technologies, such as solvents with lower heats of regeneration and lower cost equipment compared with the current technically viable options. The PC4 provides a wide range of process conditions for testing with coal-derived flue gas.

Further, the NCCC/PSDF staff will evaluate oxy-combustion as a way to significantly reduce CO_2 emissions from coal-fired power generation. Researchers at the NCCC will build on their previous operational experience with the Transport Reactor to investigate the economic feasibility of operating it as an oxygen-blown, pressurized, circulating fluid bed combustor. The research to be completed includes engineering studies to compare the Transport Reactor oxy-combustion process to other power plant options.

Finally, work will continue in developing technologies specifically related to coal gasification processes. While the previous successful testing of the PSDF gasification process has led to commercialization of several processes (e.g., the Transport Gasifier and continuous fine ash removal systems), important work remains to make IGCC processes more reliable, efficient, and

commercially viable. Including CO_2 capture in advanced coal power plants will increase the plant cost of electricity, so opportunities to reduce cost in every part of the gasification process will be pursued. The considerable on-site expertise in gasification processes as well as the unique testing opportunities afforded by the existing PSDF gasification process make continued gasification process development a logical and cost-effective undertaking.

In partnership with the DOE, the NCCC/PSDF established and met the milestones listed in Table 1 during Budget Period Two (BP2).

Table 1. Major Project Milestones for Budget Period Two.

Research Area	Milestone	Planned Completion Date	Actual Completion Date	Report Reference Section
Gasification	Conduct gasification test run R03	Nov 2009	Dec 2009	5.0
Pre-Combustion	Support membrane testing	Dec 2009	Dec 2009	3.4
Oxy-Combustion	Evaluate commercial feasibility of Transport Reactor in oxy-combustion mode in preliminary screening	Jan 2010	Jan 2010	2.2
Post-Combustion	Complete design of Pilot Solvent Test Unit (PSTU) and associated BOP infrastructure	Mar 2010	Mar 2010	4.2
Pre-Combustion	Complete first phase of SCU infrastructure upgrades	Mar 2010	Mar 2010	3.1
Fuel Flexibility	Perform off-line test with different biomass/coal	Mar 2010	Mar 2010	5.2.1
Gasification	Conduct R04 test run	Apr 2010	Apr 2010	5.0
Fuel Flexibility	Co-feed biomass with coal for 100 hours test	Jun 2010	Apr 2010	5.2
Support	Complete annual technology screening and set BP3 priorities	Jun 2010	Jun 2010	2.1
Post-Combustion	Receive and install modular PC4 utility pipe bridge and begin receiving modular PSTU	Jun 2010	Jun 2010	4.1
Pre-Combustion	Complete second phase of SCU infrastructure upgrades	Jun 2010	Jun 2010	3.1
Gasification	Conduct R05 test run	Aug 2010	Aug 2010	5.0
Pre-Combustion	Perform tests with new water-gas shift catalysts to lower steam-to-CO ratios	Sep 2010	Sep 2010	3.2
Post-Combustion	Install modular PSTU	Sep 2010	July 2010	4.1
Post-Combustion	Complete PSTU and continue post-combustion BOP construction	Nov 2010	Nov 2010	4.1
Fuel Flexibility	Continue improvements in PDAC coal feeder performance, including reducing feed perturbations and increasing solid-to-gas ratios	Dec 2010	Sept 2010	5.1
Oxy-Combustion	Evaluate commercial feasibility of Transport Reactor in oxy-combustion mode by completing detailed system studies and economic analysis	Dec 2010	Dec 2010	2.2
Post-Combustion	Begin PSTU commissioning	Dec 2010	Dec 2010	4.2.2

Project Partners. Southern Company Services manages and operates the facility, and other project participants include the Electric Power Research Institute and leaders in the power and coal industries, including American Electric Power, Luminant, NRG Energy, Arch Coal, Peabody Energy, and Rio Tinto.

2.0 TECHNOLOGY ASSESSMENT

Effective technology assessment begins with a screening process to ensure that the technologies to be tested and developed have strong potential for commercial deployment. This is accompanied by preliminary economic analysis of integrated plant configurations to assess the overall process economic feasibility. After the technology is tested, data analysis and public reporting provide industry with key information for improving technology development strategies.

2.1 TECHNOLOGY SCREENING

In order to identify technologies for inclusion in the NCCC test plan, the technology screening process was developed in collaboration with DOE's National Energy Technology Laboratory (NETL).

2.1.1 TECHNOLOGY SCREENING PROCESS

Candidate technologies are evaluated using both quantitative screening criteria shown in Table 2 and qualitative screening criteria related to shared DOE and NCCC objectives and budget considerations. The factors influencing DOE/NCCC objectives include cost reduction, fuel flexibility, short-term commercial implementation, and long-term potential. Budget considerations affecting qualitative screening criteria include project funding level, cost of testing, cost of developing, and ease of accommodation.

Table 2. Quantitative Technology Screening Criteria.

Ranking Category and Scoring Criteria	Weighting Factor
I. Projected Benefits	60%
• Impact on total cost of electricity	
• Impact on energy consumption	
• Impact on capital cost	
• Impact on power plant efficiency	
• CO_2 emission reduction	
II. Technology Strength	30%
• Scientific soundness of concept	
• Current status of the technology	
• Simplicity and robustness	
• Commercialization	
• Environmental soundness	
III. Organization Strength	10%
• Intellectual property/license of the technology	
• Capability of further development	
• Technical and management team	

The DOE NETL and the NCCC communicate throughout the screening process, which involves:

- Selection of a technology developer from a technology pool
- Evaluation of the selected technology developer with due diligence using criteria agreed upon by the DOE/NCCC screening team
- Establishment of non-disclosure agreements with the selected developer in order to receive detailed information
- Recommendation by the DOE and NCCC screening team after review of a technology evaluation report written by the NCCC staff
- Finalization of legal and engineering documentation for the projects and testing of the selected technology

The technology evaluation reports follow the format given in Table 3 and include a scoring system. After reviewing the report, the screening team (see Table 4) decides whether to include it in the NCCC test plan. Since the information in the technology evaluation reports is confidential, the reports are held at the NCCC site and are available for DOE review.

Table 3. Format for the NCCC Technology Evaluation Report.

1. Introduction
2. Technology Summary
3. Technology History
3.1. Test Results
3.2. Future Test Plans
3.3. Pathway to Commercialization
4. Projected Benefits
5. Technology Strength
6. Organizational Strength
7. Summary

Table 4. Technology Screening Team.

DOE/NETL	NCCC/PSDF
Jared Ciferno	Doug Maxwell
John Litynski	Frank Morton
Michael Matuszewski	John Wheeldon
Morgan “Mike” Mosser	Tony Wu
George ”Geo” Richards	

2.1.2 TECHNOLOGY SCREENING RESULTS

In December 2010, the technology screening team met to discuss the evaluations of technologies from Babcock & Wilcox (B&W), Aker Solutions, and Chiyoda Corporation. After presentation of the evaluations by the NCCC and discussion among the group, NETL agreed with the NCCC proposal to incorporate testing by B&W, Aker, and Chiyoda into the NCCC test plan.

Babcock & Wilcox. B&W is developing a post-combustion CO_2 capture process based on amine solvents. The group has screened many solvents at a lab scale at the company’s R&D center in Barberton, Ohio, and has verified the lab results on five amine solvents at its 0.3 MW pilot plant.

B&W proposes to test its best performing solvent at the NCCC. The selected solvent will be provided by the University of Texas.

Aker Solutions. Aker is developing a post-combustion CO_2 capture process based on amine solvents. Aker has refined its process in progressively larger tests from lab scale up to a 1.0 MW, self-contained mobile test unit that includes process equipment and controls. Aker proposes to test its best performing solvent in the test unit with flue gas from the PC4 in 2011.

Chiyoda Corporation. Chiyoda is developing a post-combustion CO_2 capture process based on amine solvents. Chiyoda has screened many solvents and proposes to test its best performing solvent in the PC4 in late 2011 or early 2012.

2.2 ECONOMIC AND ENGINEERING STUDIES

In 2009, researchers at the NCCC conducted a screening level engineering and economic study to estimate the performance and cost for a proposed advanced power generation system using the Transport Reactor in a pressurized oxy-combustion system to produce electric power and sequestration-ready CO_2. Results of this screening-level analysis of the Transport Oxy-Combustion (TROC^{TM}) system were described in the Budget Period One Topical Report and showed that the technology holds considerable promise and warrants further development and study. Because of these positive preliminary results from the screening study, a more detailed engineering economic evaluation was performed in BP2.

During the BP2 reporting period, staff compiled a study entitled "Engineering Assessment of Retrofit and Repowering Options for CO_2 Capture at a Pulverized Coal Plant." The purpose of the study was to evaluate the economic prospects of CO_2 capture from an existing mid-size coal-fired power plant by either retrofitting the plant with post-combustion CO_2 capture or by repowering the plant with the TROC technology. The results of the study will guide research and development of CO_2 capture technologies at the NCCC.

2.2.1 STUDY BASIS

Two technologies were evaluated for CO_2 capture repowering and retrofit of a sub-critical 250 MW pulverized coal (PC) unit: post-combustion capture and oxy-combustion. The base case in the study adds the following post-combustion technologies to the PC unit:

- Selective catalytic reduction (SCR) to reduce NOx to less than 0.03 lb/MMBtu on a higher heating value (HHV) basis
- Baghouse to capture mercury and aerosols while reducing particulates below 0.01 lb/MMBtu
- Flue gas desulfurization (FGD) to capture more than 98 percent of the flue gas SO_2
- CO_2 capture, drying, and compression systems to capture 90 percent of the CO_2 and produce 99.99 percent pure product CO_2

Five cases of TROC, a pressurized oxy-combustion process being evaluated at the NCCC, were investigated. This technology inherently controls particulate, NOx, SOx, and CO_2 without the addition of pollution control equipment such as SCR or FGD systems. Four cases were

examined in this study to investigate different CO_2 purification options delivering varying levels of product CO_2 purity. A fifth case investigated the financial effects of repowering at a more compact site, i.e., one with a smaller footprint. Table 5 summarizes the six study cases.

Table 5. Retrofit and Repowering Study Cases.

	Technology
Base Case (PCC)	Post-combustion capture
Case 1	TROC with no CO_2 purification
Case 2	TROC with O_2 scavenging
Case 3	TROC with partial condensation
Case 4	TROC with distillation
Case 5	Case 4 at a compact site

2.2.2 METHOD OF STUDY

A representative site for repowering and retrofit was selected from among the Southern Company generating plants as the basis for this study. It holds two nominal 250 MW coal units with low-NOx burners, over-fire air, and precipitators that burn bituminous coal to drive a 2,400 psia / 1,000°F / 1,000°F steam cycle.

Capital costs for the post-combustion capture case SCR, baghouse, FGD, and CO_2 capture systems were estimated building on vendor quotes, while estimates for the required interconnections and added balance of plant systems were developed by Southern Company Services. Operating costs were calculated based on existing plant costs and adding the additional personnel, capital repairs, and consumables required for the new systems, or by using a factor of capital supplied by a system vendor.

For the TROC cases, the air separation unit (ASU) and CO_2 compression and purification unit (CPU) capital costs were supplied by a vendor (on a turnkey basis), the TROC island costs were scaled from Southern Company data on similar systems, and the interconnections and new balance of plant systems were estimated by Southern Company Services. Operating costs were estimated in the same manner as for the post-combustion capture case.

The expected error band on the capital costs is ±25 percent based on the level of engineering work completed. Since a large majority of the equipment is common to all cases, comparative costs are more accurate than the error band given above. All costs are presented in January 2010 dollars.

Detailed heat and material balances were completed for all cases utilizing original equipment performance data from the PC unit steam cycle. These include compressing the product CO_2 to 2,200 psia at the plant boundary. Different options for integrating the new technologies with the existing steam cycle were investigated, and each case was optimized for cost and performance.

Preliminary site layouts were also completed to ensure that all systems fit in the available space. For Case 5, it was assumed that expansion space was not available at the site, so costs were

added for boiler and precipitator demolition to make room for the TROC island and CPU. For this case, costs were also added to reflect locating the ASU at a stand-alone site one mile away.

2.2.3 DESCRIPTION OF POST-COMBUSTION CAPTURE CASE

The SCR system is integrated into the existing boiler between the precipitators and the air heater. An economizer bypass was included to maintain SCR temperatures during partial load operation. After the air heater, the flue gas flows through the existing induced draft (ID) fans, which were modified to accommodate the increased system pressure drop. Downstream of the ID fans is a new baghouse that includes an activated carbon injection system for mercury control. Axial booster fans were added downstream of the baghouse to compensate for the added pressure drop. The FGD system is located downstream of the booster fans and discharges into the CO_2 capture system. A wastewater treatment facility is included to condition the scrubber effluent. The post-combustion CO_2 capture process utilizes an advanced solvent to recover the CO_2 from the flue gas. CO_2 is stripped from the solvent using low pressure steam, is dried, and then compressed.

The steam cycle provides low pressure steam to the amine stripper reboilers, medium pressure steam to the amine reclaimers, and low pressure feedwater to the desorber condensers, bypassing the first low-pressure feedwater heater. Low pressure steam for the amine stripper reboilers is taken from the steam turbine crossover and sent through a let-down turbine to recover energy before reaching the CO_2 capture system. Since about 40 percent of the total steam flow is required for the amine stripper, the existing low pressure steam turbine is replaced by a new one that is designed to maintain the crossover pressure with the smaller remaining steam flow.

2.2.4 DESCRIPTION OF THE TROC CASES

Unlike the base case of post-combustion capture, Transport Oxy-Combustion repowers the existing steam turbine by replacing the existing boiler and emission control systems (e.g. precipitator) thereby avoiding the need for retrofit of conventional emissions control technologies. Similar to the base case, the steam cycle along with other existing auxiliary systems continue operation with some modifications.

The air separation unit (ASU) uses cryogenic distillation to deliver 96 percent pure oxygen at the required pressure for use in the TROC unit. The ASU includes liquid storage to maintain the supply of oxygen and nitrogen during upset and outage conditions.

The TROC system combusts the bituminous coal currently processed at the existing plant under pressure in the presence of oxygen, producing a gas stream of mostly CO_2 and H_2O from which heat is recovered into the steam cycle. A proprietary fluidized-bed solids cooler maintains the moderate combustion temperature by efficiently removing approximately two thirds of the heat of combustion into the steam cycle. The resulting large flow of recycled solids promotes complete combustion and allows a much lower excess oxygen level in the combustor, decreasing the oxygen in the products of combustion. Another advantage of the TROC technology is that combustion is at a pressure sufficient to allow useful heat to be recovered from the condensation of water as the products of combustion are cooled.

Emissions are largely controlled within the TROC system without the need for large post-combustion cleanup systems. Thermal NOx is limited by combusting with oxygen rather than air and at moderate temperatures. Fuel NOx formation is mitigated by the CO_2 which is recycled for fluidization. Limestone is introduced in the combustor to reduce SOx emissions, and trona is used to capture chlorine and fluorine. A fixed bed of activated carbon is used to capture any mercury. Case 2 includes the injection of coke breeze in the combustor to reduce the oxygen level in the product CO_2, while Cases 3 and 4 include downstream CO_2 purification by partial condensation and distillation, respectively, and Case 1 has no means for O_2 reduction.

The steam cycle provides small amounts of low pressure steam to the ASU and CPU and also to the coal preparation system for drying, but the main integration with the TROC system is through heat recovery and feedwater heater bypass. Low pressure feedwater is used in cooling the low-temperature products of combustion, partially bypassing all three low pressure feedwater heaters. In addition, part of the high pressure feedwater is sent from the deaerator to the high-temperature products of combustion cooler in which superheated steam is generated.

2.2.5 RESULTS

The data presented below are all for one nominal 250 MW PC unit. Table 6 compares the performance and major flows for the unmodified PC unit, a post-combustion carbon capture (PCC) retrofit, and TROC repowering.

Table 6. Performance and Major Flows With and Without CO_2 Capture.

	PC Unit	PCC Base Case	TROC Case 1	TROC Case 2	TROC Case 3	TROC Cases 4&5
Gross Power, MW	274.0	246.9	279.8	280.0	279.3	279.5
	--	-10%	+2%	+2%	+2%	+2%
Auxiliary Load, MW	19.6	59.5	85.1	84.5	84.0	85.0
Net Power, MW	254.4	187.4	194.6	195.4	195.3	194.5
	--	-26%	-24%	-23%	-23%	-24%
HHV Heat Input, MMBtu/hr	2,406	2,409	2,262	2,264	2,262	2,269
HHV Heat Rate, Btu/kWh	9,460	12,860	11,620	11,580	11,580	11,660
	--	+36%	+23%	+22%	+22%	+23%
HHV Net Efficiency, %	36.1	26.5	29.4	29.5	29.5	29.3
Coal, k lb/hr	186.1	186.3	174.9	173.1	174.9	175.5
Coke Breeze, k lb/hr	0	0	0	2.0	0	0
Oxygen, k lb/hr	0	0	423.7	420.5	423.7	425.2
Limestone, k lb/hr	0	5.9	7.2	7.1	7.2	7.2
Trona, k lb/hr	0	0	0.15	0.15	0.15	0.15
Makeup Water, k lb/hr	0	763.8	363.7	363.6	359.6	364.8
Demineralized Water, k lb/hr	18.2	18.1	18.1	18.1	18.1	18.1
CO_2 Product, k lb/hr	0	458.6	496.1	493. 9	439.0	428.6
Stack Gas/Off Gas, k lb/hr	2,784	2,264	5.3	5.2	62.4	75.1
Ash, k lb/hr	18.5	22.1	27.6	27.5	27.6	27.6
Gypsum*, k lb/hr	0	49.7	0	0	0	0

* 21% solids, by weight

Both PCC and TROC negatively affect the net capacity and efficiency of the unit, with the TROC cases having about a third less impact. The performance and flows of the different TROC cases are almost identical.

The PCC case requires significantly more makeup water to the cooling tower because of the cooling loads in the post-combustion CO_2 capture system. The other major difference is that the TROC cases have almost no stack gas or off gas compared with the PC unit and PCC case.

CO_2 Recovery and Product Purity. The CO_2 capture percentage and CO_2 product purity for the technologies evaluated in this study are summarized in Table 7.

Table 7. CO_2 Recovery and Product Purity for Study Cases.

	PCC Base Case	TROC Case 1	TROC Case 2	TROC Case 3	TROC Cases 4 & 5
CO_2 Capture, %	90.0	99.0	99.0	90.0	90.0
Vol % CO_2 in Product CO_2	99.99	93.55	94.50	96.65	99.99
Vol % O_2 in Product CO_2	< 0.004	1.01	0.05	0.49	0.00
Vol % of N_2 in Product CO_2	< 0.01	1.42	1.42	0.59	0.00
Vol % of Ar in Product CO_2	0.00	4.00	4.00	2.24	0.01
Vol % of H_2O in Product CO_2	< 0.01	0.00	0.00	0.00	0.00
ppmv of SOx in Product CO_2	< 10	1	1	2	0
ppmv of NOx in Product CO_2	< 10	100	20	114	11

The PCC case and TROC Cases 4 and 5 give a high purity that meet published CO_2 purity specifications and should be suitable for any use, although at only 90 percent CO_2 capture. A range of lower purities (which may be suitable for sequestration) and higher CO_2 capture levels are available in TROC Cases 1 through 3.

Cost of Electricity. Table 8 shows the levelized costs of electricity (LCOE) for a nominal 250 MW plant and summarize other major results for PCC and TROC. These cases use a capacity factor of 75 percent.

Table 8. Levelized Cost of Electricity for All Study Cases.

	PCC Base Case	TROC Case 1	TROC Case 2	TROC Case 3	TROC Case 4	TROC Case 5
Plant Output, MW	187.4	194.6	195.4	195.3	194.5	194.5
Heat Rate, Btu/kWhr, HHV	12,860	11,620	11,580	11,580	11,660	11,660
Total Plant Cost, MM$	790	727	729	753	775	798
Total Plant Cost, $/kW	4,220	3,730	3,730	3,860	3,980	4,100
Fixed O&M, $/kW-yr	117.8	88.6	88.6	90.4	92.4	92.4
Variable O&M, mills/kWh	8.63	3.06	3.64	3.05	3.07	3.07
Capital, mills/kWh	91.2	80.7	80.6	83.4	86.1	88.7
O&M, mills/kWh	26.6	16.5	17.1	16.8	17.1	17.1
Fuel, mills/kWh	21.1	19.1	19.0	19.0	19.1	19.1
LCOE, mills/kWh (2010$)	138.8	116.3	116.7	119.2	122.3	124.9

The TROC cases have a total plant cost of 3 to 12 percent less than the PCC case on a $/kW basis, but this is not considered significant based on the estimating accuracy of this study. The TROC compact site sensitivity (Case 5) adds approximately 3 percent to the capital cost, so the costs of repowering a more compact site are not prohibitive. The TROC cases have a significant advantage in O&M costs (36 to 38 percent lower), primarily due to the amine solvent makeup costs in the PCC case, and a slightly lower fuel cost, which is a direct result of the heat rate difference between PCC and TROC. These differences combine to give TROC a 10 to 16 percent lower levelized cost of electricity, assuming the same dispatch rate and capacity factor. Figure 2 plots the LCOE.

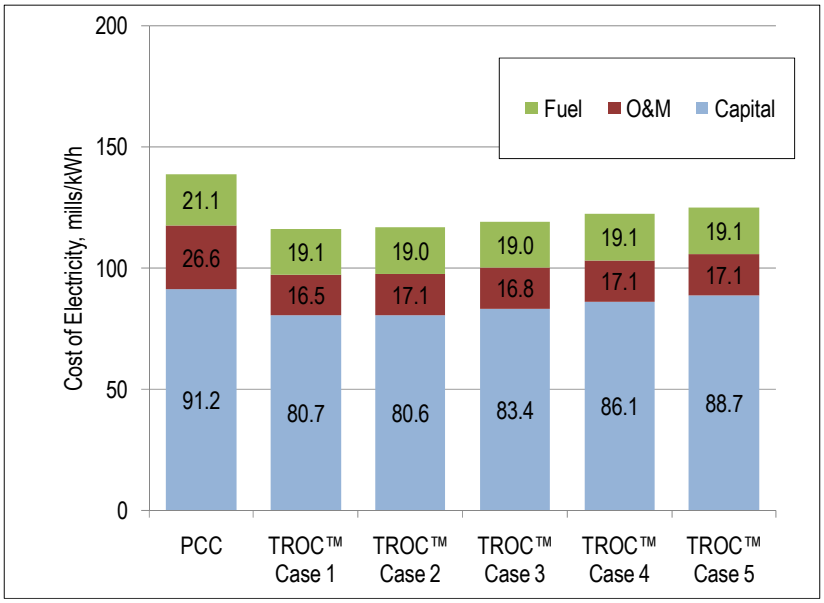

Figure 2. Levelized Cost of Electricity at 75 Percent Capacity Factor for All Study Cases.

Cost of Electricity Sensitivity to Capacity Factor. Although the total plant costs are similar for PCC and the TROC cases, the costs to dispatch the plant and produce a unit of power (the sum of the fuel cost plus the variable O&M cost) are significantly different as listed:

- PCC Base Case – 29.7 mills/kWh
- Case 1 – 22.1 mills/kWh
- Case 2 – 22.6 mills/kWh
- Case 3 – 22.0 mills/kWh
- Case 4 – 22.2 mills/kWh
- Case 5 – 22.2 mills/kWh

This suggests that in operation, the TROC plants would be operated at a higher capacity factor, which would lead to a lower levelized cost of electricity. Figure 3 demonstrates the LCOE sensitivity to capacity factor.

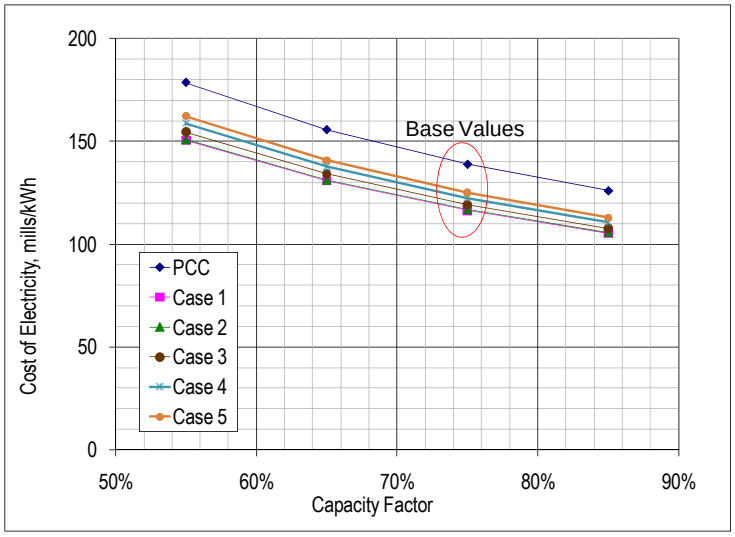

Figure 3. LCOE Sensitivity to Capacity Factor.

If a PCC plant were dispatched to have a capacity factor of 55 or 65 percent, the levelized cost of electricity from Figure 3 would be about 156 to 179 mills/kWh. In contrast, if a TROC plant were dispatched at a capacity factor of 85 percent, its LCOE would be 105 to 113 mills/kWh, or about 30 to 40 percent less than for PCC. Therefore, the difference in variable O&M costs and fuel costs would produce significant differences in the actual LCOE.

2.2.6 COSTS OF CO_2 CAPTURE AND AVOIDANCE

Table 9 provides the costs of CO_2 capture and of CO_2 emissions avoided for all cases.

Table 9. Costs of CO_2 Capture and Emissions Avoided for All Study Cases.

	PCC	TROC Case 1	TROC Case 2	TROC Case 3	TROC Case 4	TROC Case 5
Cost of CO_2 Capture, $/ton	64	46	47	54	56	59
Cost of CO_2 Capture, $/tonne	71	51	52	59	62	65
Cost of CO_2 Emissions Avoided, $/ton	88	55	56	65	69	72
Cost of CO_2 Emissions Avoided, $/tonne	97	61	61	72	76	79

The advantage of capturing 99 percent of the CO_2 at lower purity rather than 90 percent at higher purity becomes evident in the results for Cases 1 and 2, since they have significantly lower costs of CO_2 capture and CO_2 avoidance than the other cases. The higher LCOE of the PCC case is reflected above, with CO_2 capture and avoidance costs 8 to 60 percent higher than for TROC.

2.2.7 CONCLUSIONS

This study investigated two options for mitigating emissions at a representative existing mid-sized coal plant. For the system arrangements considered, using bituminous coal, the results showed the following:

- Both PCC and TROC require a significant capital investment and negatively affect plant performance.
- Both PCC and TROC are capable of recovering a minimum of 90 percent of the CO_2 produced by the plant, and some TROC configurations can capture 99 percent if the CO_2 product purity is decreased.
- Both PCC and TROC (in one configuration) are capable of meeting typical industry CO_2 product specifications, including some for enhanced oil recovery.
- If high product purity is not required, the TROC capital cost can be reduced by choosing a configuration with less CO_2 purification, while still achieving a purity sufficient for sequestration.
- Although the results show 3 to 12 percent lower capital costs for TROC compared with PCC (on a $/kW basis), the difference is within the accuracy of the estimate.
- Although a space-constrained site adds to the capital cost of TROC, Case 5 suggests that the increment is not excessive.
- TROC has lower heat rates and O&M costs compared with PCC resulting in a 10 to 16 percent lower LCOE, at 75 percent capacity factor, and this advantage widens if dispatch differences are considered.
- It is expected that PCC and TROC dispatch rates would be significantly different since the TROC dispatch costs (fuel plus variable O&M) are 24 to 26 percent lower than for PCC.

3.0 PRE-COMBUSTION CO_2 CAPTURE AND SEPARATION

To advance pre-combustion CO_2 capture technologies, the NCCC has the capacity to investigate key processes including gas/liquid contacting systems, solvents for CO_2 capture/separation, water-gas shift processes, and emerging syngas processes. The infrastructure for pre-combustion CO_2 capture testing provides for a wide range of test conditions, and includes the Syngas Conditioning Unit (SCU). During BP2, the SCU was modified, and various CO_2 capture and water-gas shift tests commenced, as did support of gas separation membrane testing by outside researchers.

3.1 SYNGAS CONDITIONING UNIT

The SCU is a flexible slipstream facility that can accommodate multiple, small-scale tests, such as water-gas shift, hydrolysis, desulfurization, and CO_2 capture. The SCU, shown in Figure 4, consists of small reactor vessels, arranged to allow operation in series or in parallel, which accommodate a range of flow rates, temperatures, and pressures. The unit is also used to support outside technology developers by providing a syngas test location, and it has supported development of technologies such as gas separation membranes, fuel cells, and heavy metal removal processes.

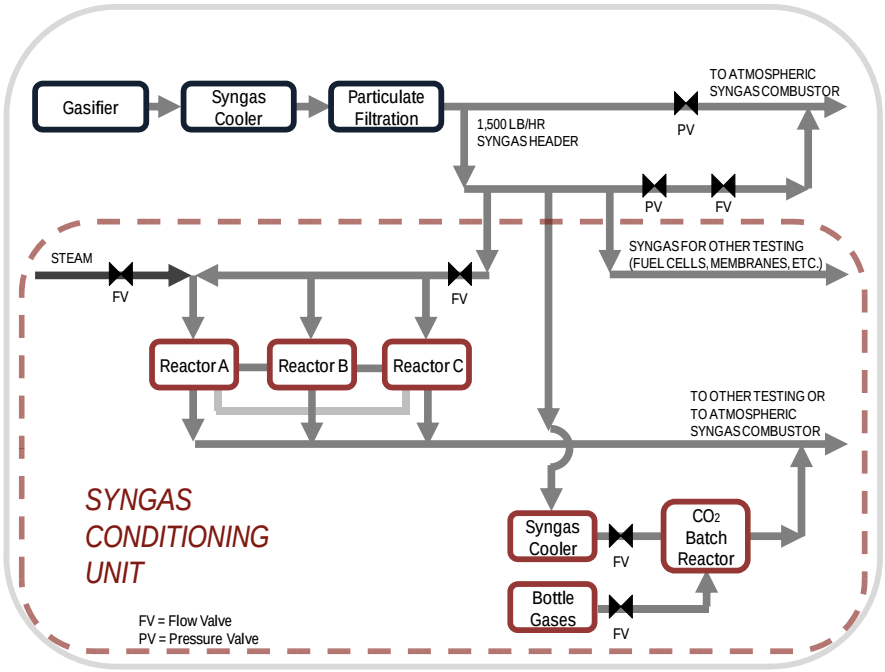

Figure 4. Flow Diagram of the Syngas Conditioning Unit.

SCU Modifications. Upgrading the SCU continued during BP2 to accommodate the ever-expanding range of technology development. A new gas analyzer building for the SCU was installed during BP2 to house existing and future analysis equipment. The existing analyzers include six gas chromatographs (GCs), four continuous syngas analyzers, one Fourier Transform Infrared (FTIR) analyzer, four area gas detectors, and two calibration panels.

Views of the outside and inside of the building are presented in Figure 5. The syngas sample lines are routed from the SCU test equipment along with lines for calibration gases, GC nitrogen carrier gas, and instrument air. The system has over 40 sample and calibration connections and the analyzer outputs are connected to the Plant Information data acquisition system.

Figure 5. Gas Analyzer Building for the Syngas Conditioning Unit.

Other modifications made to the SCU, which comprised Phase I and Phase II infrastructure improvements, included:

- New instrumentation (including a flow meter, control valve, and local instrumentation) and changes to associated piping and heat tracing to support higher syngas flow rates for mercury sorbent testing
- Accommodations for a mass spectrometer supplied by NETL to validate the design of the analyzer system used to monitor the performance of the Johnson Matthey mercury sorbent
- Modifications to existing thermocouples and addition of new thermocouples to improve measurements of temperature profiles in the water-gas shift (WGS) fixed-bed reactor and at the reactor outlet
- Addition of probes to measure moisture content at the inlet of the WGS reactors
- Installation of heat tracing to eliminate steam condensation in the steam supply sub-header to the WGS reactors
- Addition of a new model syngas chromatograph
- Modifications to the temperature control on the syngas piping to the Membrane Technology & Research (MTR) membrane skid to maintain a stable syngas feed temperature
- Addition of intrinsically safe nitrogen purges to the Media & Process Technology (MPT) membrane skid electronic and variac enclosures

3.2 WATER-GAS SHIFT CATALYST TESTING

Evaluation studies completed at the NCCC show that catalyst vendors generally recommend high steam-to-CO ratios to maximize CO conversion and minimize methane formation. Values as high as 2.6 have been quoted. This is based on requirements by chemical production processes to maximize hydrogen formation (the desired product) and minimize methane formation, a

potential contaminant. High steam content also suppresses carbon formation from the cracking of long-chain hydrocarbons. For power plant applications, where the objective may be to capture only 90 percent of the CO_2, incomplete conversion of CO and the production of some methane are acceptable. Moreover, there are little, if any, long-chain hydrocarbons in coal-derived syngas so there is no need for excess steam to suppress carbon formation.

The evaluation studies also indicated that for a 500-MW IGCC plant, a steam-to-CO ratio of 0.1 corresponded to 4 MW of power, so operating with excess steam would have a significant impact upon net power production. For example, if a steam-to-CO ratio of 1.6 was acceptable rather than 2.6, then an additional 40 MW would be available.

To determine the feasibility of operating with steam-to-CO ratios lower than those normally proposed, the NCCC began investigating the performance of WGS catalysts provided by the major suppliers. The terms of the confidentiality agreements signed prevent identification of the catalysts in this report.

Test Procedure. The inlet and outlet gas compositions were determined using the gas chromatography and non-dispersive infrared (NDIR) instruments. The inlet flow rates of syngas and steam were measured using a V-cone meter and orifice plate, respectively. The accuracy of these meters was checked using known flows of nitrogen prior to the start of the run and during the run. The outlet flow rate was not measured but was calculated using nitrogen present in the syngas as a marker. Using the instrumentation available, the composition of the syngas entering and leaving the WGS reactor were calculated on both dry and wet bases.

For testing during gasification test run R05, an amount of 13 pounds of catalyst was installed in the vessel, giving a fixed bed 26-inches deep supported on a 310 stainless steel mesh. The syngas and steam flowed vertically downward through the catalyst. The gas flow rates were held constant during the run to maximize the data collected for a given space velocity. The heat tracing on the line from the header to the vessel was adjusted to achieve an inlet temperature of 540°F to keep the exit temperature below 650°F, above which sintering could occur. The parameter that varied the most was the steam-to-CO ratio. Table 10 lists the test conditions for R05.

Table 10. Water-Gas Shift Catalyst Test Conditions.

Test Parameter	Nominal Values
Syngas Flow Rate, lb/hr	50
Steam Flow Rate, lb/hr	2.0
Operating Pressure, psia	195
Inlet Temperature, °F	540
Superficial Syngas Velocity, ft/s	0.22
Space Velocity, hr^{-1}	3,240
H_2O/CO Molar Ratio	0.8 to 1.6
Test Duration, hours	780

To monitor how the temperature varies in the catalyst bed as the WGS reaction proceeds, thermocouples were installed along the reactor length. Figure 6 plots the temperatures for select operating periods at the six locations. The maximum temperature occurred at the 3-inch level. The temperature drop for the lower two thermocouples was attributed to heat losses from the flange, which is only insulated and not heat traced as is the reactor wall section. The mean temperature increase in the reactor was 90°F from 530 to 620°F; without the heat loss, the temperature increase would have been closer to 95°F.

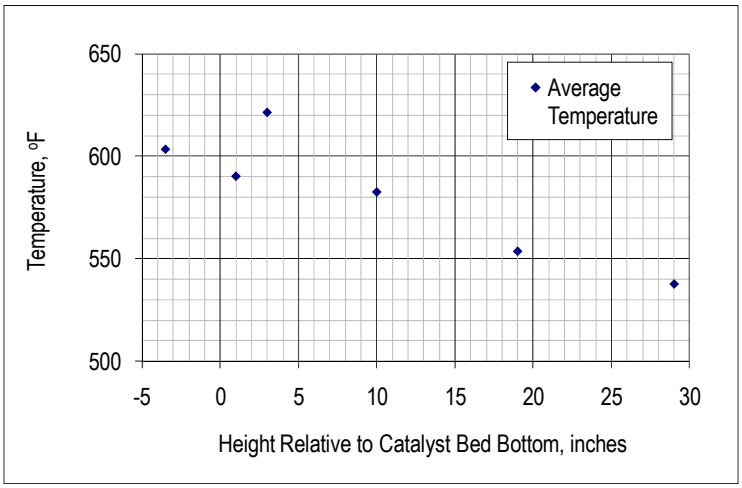

Figure 6. Temperature Profile in the Fixed Bed Reactor during R05.

The mean values for the major syngas components during R05 are given in Table 11 along with the analyzer used to make the determination. Each analyzer has its own error bias which data analysis accentuates when comparing the changes in composition between the inlet and outlet of the reactor.

Table 11. Mean Syngas Compositions at Water-Gas Shift Reactor Inlet and Outlet.

	CO	CO_2	H_2	CH_4
Inlet Concentration, vol % (analyzer used)	9.7 (NDIR)	9.7 (NDIR)	7.1 (GC)	1.02 (GC)
Outlet Concentration, vol % (analyzer used)	3.6 (GC)	14.3 (GC)	12.7 (GC)	1.04 (GC)

Figure 7 compares the amounts of CO shifted (delta CO) to the amount of CO_2 formed (delta CO_2) by the WGS reaction. These amounts should be equimolar, one mole of CO being converted to one mole of CO_2 formed, according to the water-gas shift equation:

$$CO + H_2O \leftrightarrow CO_2 + H_2 \quad \text{(water-gas shift equation)}$$

All but one data point fell within 10 percent of perfect agreement, which validated the data quality.

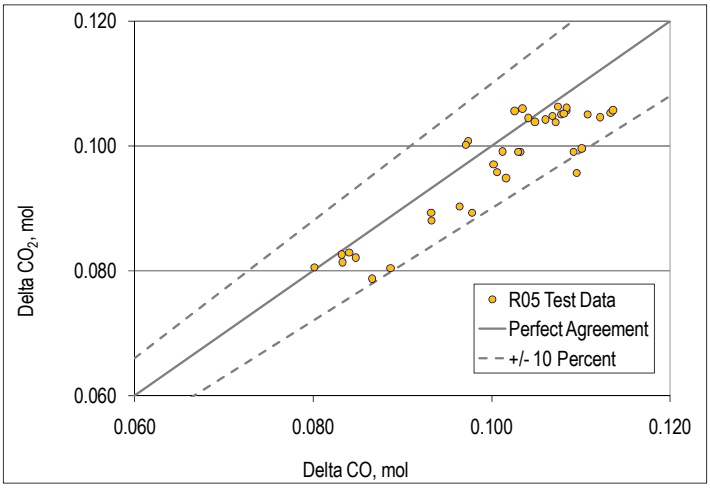

Figure 7. Amount of CO_2 Produced Compared to Amount of CO Shifted.

Figure 8 plots the amounts of CO shifted to H_2 by the WGS reaction. Again, according to water-gas shift equation, these amounts should be equimolar. The data for hydrogen did not agree as well as that for the carbon dioxide, with the data showing more hydrogen formed than CO consumed. The discrepancy likely arose from small measurement errors. Efforts continue to reduce error as much as possible.

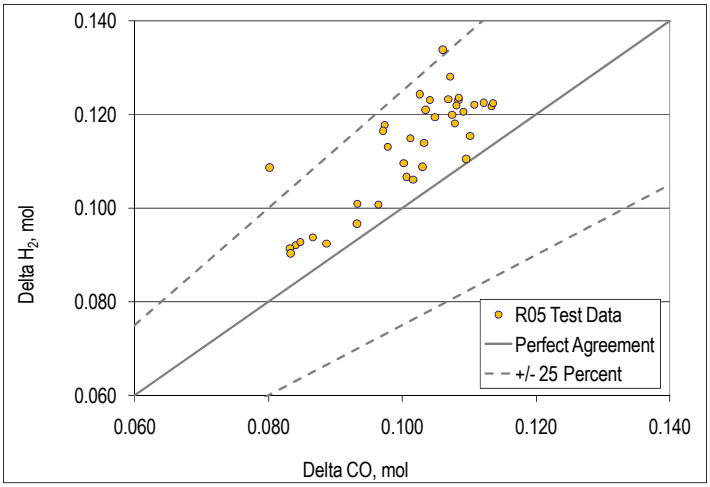

Figure 8. Amount of H_2 Produced Compared to Amount of CO Shifted.

Figure 9 compares the amount of methane entering and leaving the WGS reactor. The data showed some scatter but did not indicate that methane formation occurred. Further, carbon deposits were not detected on either the surface of the catalyst or the inside surface of the reactor.

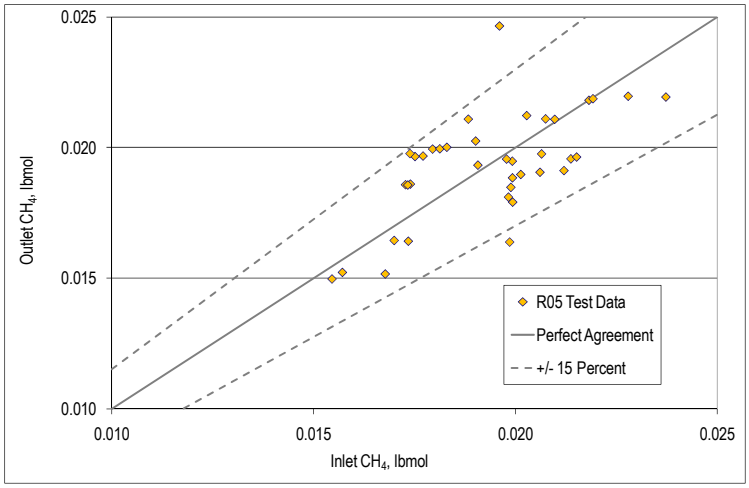

Figure 9. Comparison of Methane Content Entering and Exiting the WGS Reactor.

Figure 10 presents data showing the measured CO conversion variation with steam-to-CO ratio. Also presented is the equilibrium conversion calculated from information provided by the catalyst vendor. On average, the measured conversions were 70 percent of the equilibrium values. The trend for both data sets appeared to be asymptotic, with conversions leveling off for molar ratios greater than 1.6.

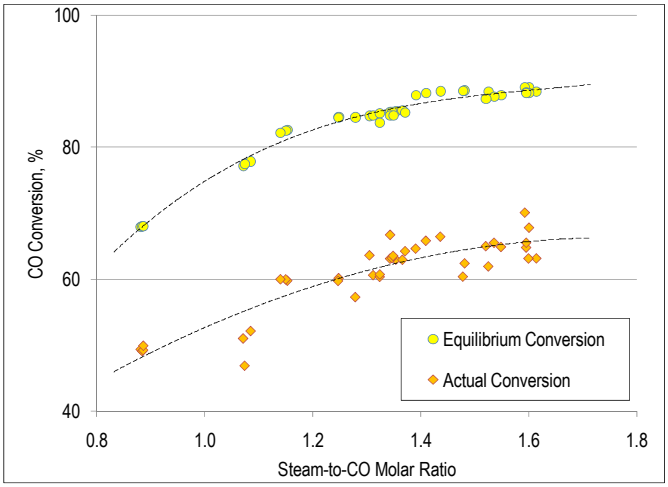

Figure 10. Comparison of Actual and Equilibrium WGS Conversions.

The tests showed that sufficiently high CO conversions were achieved at lower than recommended steam-to-CO ratios and that only marginal increases in conversion would be realized for ratios above 1.6. No methane was formed and no carbon was deposited in the reactor. For power generation applications, steam-to-CO ratios lower than those recommended for chemical production applications are acceptable.

3.3 CO_2 CAPTURE TESTING

During the reporting period, NCCC researchers investigated several CO_2 capture sorbents, including ammonia; polydimethylsiloxane, which was compared to the well-documented solvent dimethyl ether of polyethylene glycol (DEPG); and potassium carbonate and potassium prolinate, which were compared to ammonia.

3.3.1 AMMONIA CHEMISTRY

Ammonia Compounds for CO_2 Capture. Ammonia can capture CO_2 by two main mechanisms, one involving ammonium carbonate, and the other ammonium carbamate.

The carbonate route involves the following reactions:

$$NH_3 + H_2O + CO_2 \leftrightarrow (NH_4)_2CO_3 \quad (-24.1 \text{ kcal/g-mol};\ -986 \text{ Btu/lb } CO_2) \quad \text{Equation 1}$$

$$(NH_4)_2CO_3 + H_2O + CO_2 \leftrightarrow 2NH_4HCO_3 \quad (-6.36 \text{ kcal/g-mol};\ -260 \text{ Btu/lb } CO_2) \quad \text{Equation 2}$$

The carbamate route involves the following reactions:

$$2NH_3 + CO_2 \leftrightarrow (NH_3)_2CO_2 \quad (-17.7 \text{ kcal/g-mol};\ -725 \text{ Btu/lb } CO_2) \quad \text{Equation 3}$$

$$(NH_3)_2CO_2 + 2H_2O + CO_2 \leftrightarrow 2NH_4HCO_3 \quad (-12.75 \text{ kcal/g-mol};\ -521 \text{ Btu/lb } CO_2) \quad \text{Equation 4}$$

If the ammonium bicarbonate (ABC) crystallizes, heat is released, the heat of crystallization being -6.78 kcal/g mol (-277 Btu/lb CO_2). Similarly, heat is required to dissolve the crystals.

If the liquor to be regenerated contains crystals, then heat must be applied to dissolve the crystals. If the ABC releases its CO_2 to form carbonate, the heat of reaction (-260 Btu/lb CO_2) is lower than if carbamate is formed (-521 Btu/lb CO_2). Hence, it is important to know the exact chemical route followed. In addition, the formation of crystals may be beneficial in reducing the heat of regeneration. The crystals can be separated from the liquor, lowering the water content of the ABC-rich liquor sent to the regenerator, thereby lowering the sensible heat requirement. However, this will be offset to some degree by the heat required to dissolve the crystals. A comprehensive model to predict ammonia chemistry is required to resolve these issues.

The thermodynamic software identified was supplied by OLI Systems and is used widely to predict the properties for a range of aqueous solutions. When used to predict the capture of CO_2 using ammonia, the calculations are based on carbamate being the primary product of the reaction. To confirm that this is correct and validate the model, tests were completed in the SCU batch reactor to produce ammonia liquors with a range of compositions. These solutions were analyzed using nuclear magnetic resonance (NMR) spectroscopy.

The NMR technique beams an electromagnetic pulse at the solution and the energy radiated back is influenced by the properties of the molecule's nucleus. A spectral output signal is presented in Figure 11, the frequency shift being a characteristic of the nucleus and the height of the peak

being an indication of the amount present. The instrument can be programmed such that the peak value represents the percentage of the species present in solution.

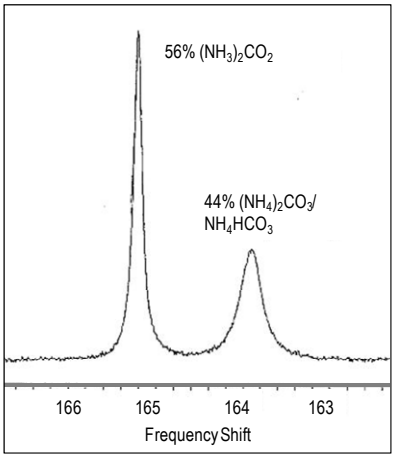

Figure 11. Output Signal from NMR Analyzer.

The left-hand peak results only from ammonium carbamate and allows direct determination of this species. The right-hand peak results from a combination of ammonium carbonate and bicarbonate requiring a means of deducing the proportions of the two species present. Research from the University of Florence showed that the greater the horizontal separation of the two peaks the greater the bicarbonate content of the left-hand peak. This group then developed a calibration curve using solutions with known carbonate and bicarbonate contents. This calibration curve was used to extract the carbonate and bicarbonate information from the on-site analyses.

Fifteen tests were completed to compare the concentration of ammonium compounds measured by NMR with values predicted by OLI. Figure 12 provides plots of the ammonium carbamate, ammonium bicarbonate, and the ammonium carbonate concentrations measured by NMR versus those predicted by the OLI program.

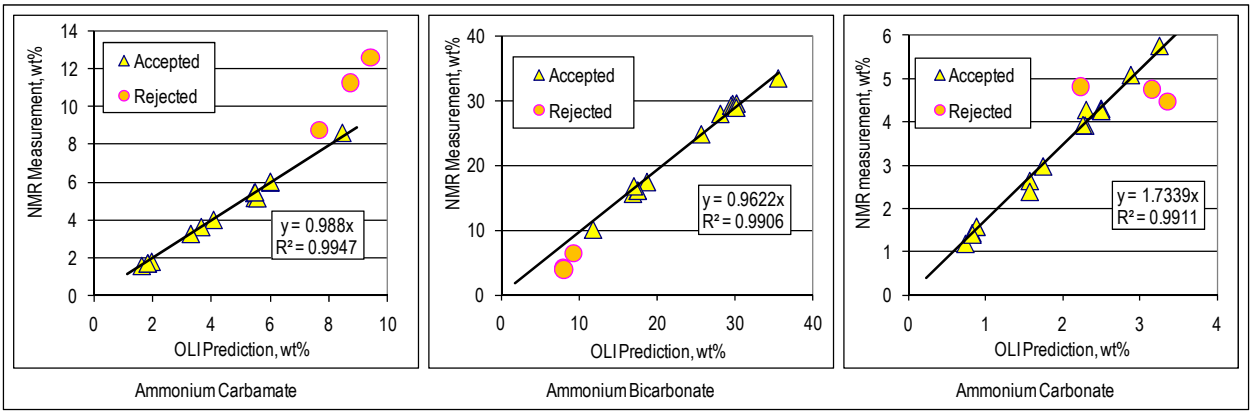

Figure 12. Comparison of Measured and Predicted Concentrations of Ammonia Compounds.

As noted in the figure, three data points were rejected from the data set. For ammonium carbamate and ammonium bicarbonate, the slope of almost one indicated good agreement. For ammonium carbonate, the measured values were appreciably higher than the predictions as indicted by the slope being greater than one. The error may have resulted from error in the calibration curve. The ABC results presented in the figure could be slightly over-predicted, giving a slope of less than one.

Adjusting the measured ABC to match the predicted value will increase the amount represented in the right hand peak of the NMR measurement and so the amount of ammonium carbonate measured is reduced. This approach improved the match achieved in the ammonium carbonate plot and lowered the slope to 1.24, but still suggested that the model under-predicts the ammonium carbonate present. It was concluded that the measured ammonium carbamate and ABC were predicted with good accuracy by the OLI model and any error associated with ammonium carbonate was low. This validated the model and allowed its use with confidence for predicting the composition of the ammonia liquor.

The model was also used to predict other performance parameters of interest. Figure 13 presents CO_2 capture data and shows that the model agreed well with the measured values. The perturbation in experimental CO_2 capture efficiency seen around 68 minutes into the test may have been related to the onset of ABC crystal formation after around 64 minutes.

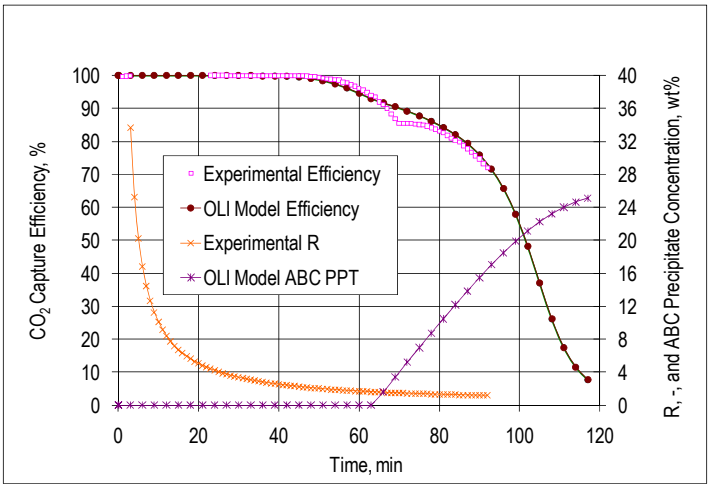

Figure 13. Comparison of Measured and Predicted CO_2 Capture Efficiencies.

The "R" value included in Figure 13 represents the ammonia-to-CO_2 molar ratio and fell as the CO_2 content of the liquor increased. When the CO_2 capture efficiency began to decrease after around 50 minutes, R was slightly greater than 2, indicating that the free ammonia was almost depleted. Up to this point, CO_2 capture occurred primarily by the reaction in Equation 3, and carbamate was the primary ammonia compound formed. After this, Equation 4 was the primary CO_2 capture reaction, and the carbamate was converted to bicarbonate. Eventually the saturation concentration was reached, resulting in the formation of ABC crystals after 64 minutes.

Figure 14 presents the concentration of ammonia exiting with the gases leaving the reactor and also shows that the model agreed well with the measured values. Ammonia was released at around 1,000 ppmv at the onset of ABC crystallization even though there was no free ammonia. This was a result of the presence of ammonia anions.

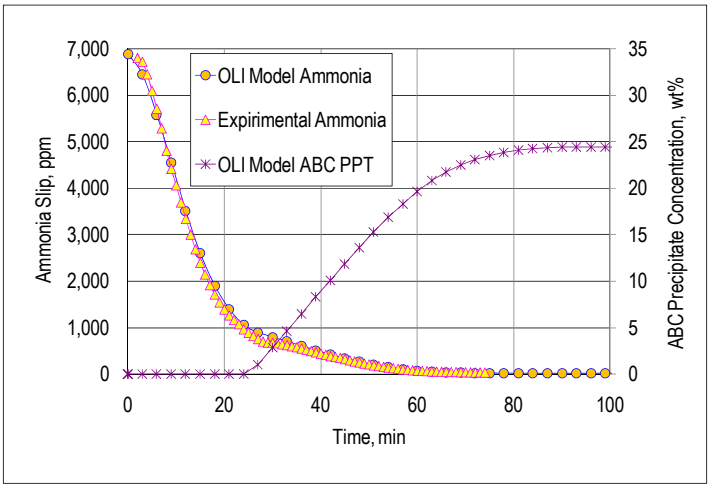

Figure 14. Comparison of Measured and Predicted Ammonia Slip.

The experimental work to date has validated the use of OLI software for predicting ammonia chemistry. Subsequent work began to identify the optimum absorber and regenerator operating conditions.

Initial Modeling Results. Initial testing using properties predicted by the validated OLI model was undertaken to determine how the composition of the liquor leaving the absorber changed as it was heated in the regenerator. The change is presented in Figure 15. This graph shows absolute values for the ammonium bicarbonate crystals and the CO_2 released, and the difference in values for the dissolved species, ammonium bicarbonate, carbamate, and carbonate.

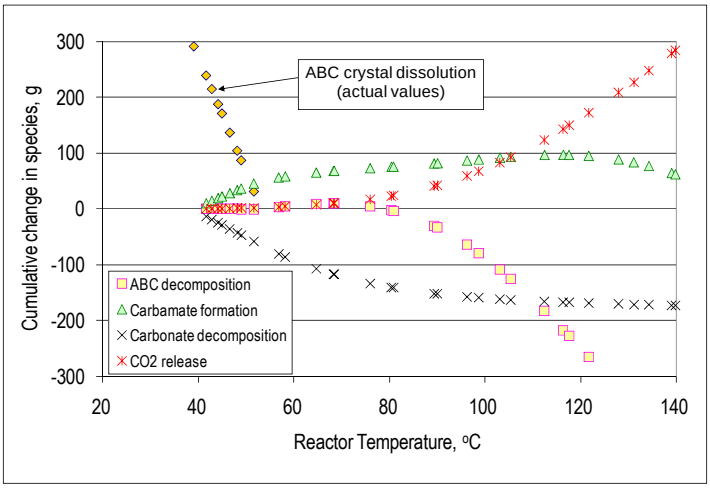

Figure 15. Change in Ammonia Liquor Composition with Reactor Temperature.

The model is based on the batch reactor to allow comparison between measured and predicted values. The 40°C data represent compositions at the end of an absorption period with 300 g of ammonium bicarbonate crystals in the liquor. As the liquor was heated, the crystals dissolved, and at 53°C, all the bicarbonate was in solution. At this temperature, 58 g of ammonium carbonate decomposed, forming 47 g of ammonium carbamate according to Equation 5, which is endothermic.

$$(NH_4)_2CO_3 \leftrightarrow (NH_3)_2CO_2 + H_2O \quad (+6.39 \text{ kcal/g-mol};\ +261 \text{ Btu/lb } CO_2) \quad \text{Equation 5}$$

Despite the temperature increase, no ammonium bicarbonate decomposed, and no CO_2 was released. Results suggest that the liquor re-established chemical equilibrium at the new temperature. At around 60°C, CO_2 release began, but ammonium bicarbonate was being formed and did not start to decompose until the temperature was around 80°C.

Controlling the absorption temperature at 40°C requires additional cooling to remove the heat released when the ammonium bicarbonate crystallizes. When regeneration is required, heat must be added to dissolve the crystals and the temperature raised to above 80°C before significant CO_2 is released. Cooling duty and water usage could be reduced if absorption could be carried out effectively closer to 60°C. This would also reduce the sensible heat required (some of which is recovered using recuperators) to raise the liquor to regeneration temperature.

A possible drawback of operating the absorber at 60°C is an increase in ammonia slip in the exiting CO_2-depleted syngas. The ammonia would be scrubbed out using water wash, although this constitutes a system loss. The feasibility of operating the absorber at temperatures greater than 40°C will be assessed with additional modeling and batch reactor testing.

Raman Spectroscope. The Raman Spectroscope employs a technique that directs a single wavelength laser beam into a solution, and the energy radiated back is influenced by the properties of the molecules present. The scattered light is collected and analyzed producing a Raman Spectrum, a representative example of which is presented in Figure 16. The species associated with the Raman shift are determined experimentally using solutions of known composition. The signal intensity is relative to that of the laser beam.

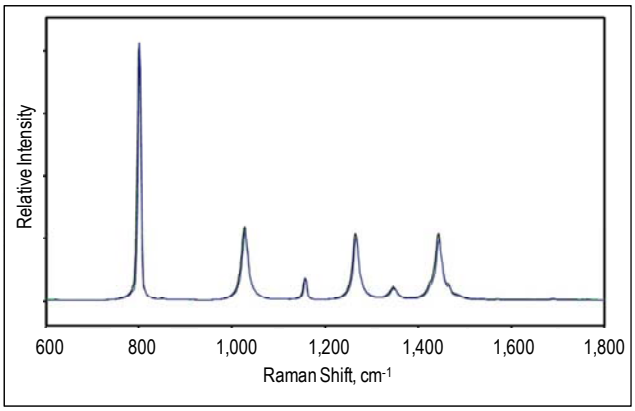

Figure 16. Example of a Raman Spectrum.

The results are obtained in real time, unlike the NMR spectroscope, which is used in the laboratory to analyze samples of the solution. Unlike the NMR peaks, the Raman peaks do not give a direct measurement of concentration, and calibration measurements are required. Some researchers have used concentrations measured using NMR to determine the value to be ascribed to the Raman peak, but this is a slow, expensive approach. As the OLI model had been validated, it was decided to use values predicted by OLI to calibrate the Raman output.

A test program was carried out in the SCU batch reactor with a Raman optical head installed in the drain line at the bottom of the vessel. Ammonium hydroxide solution (14-mole percent ammonia) was fed to the reactor, the vessel was pressurized to 300 psia, the stirrer was activated, and the temperature controller was set to 100°F. A known amount of CO_2 was bubbled through the solution after which Raman spectral data were collected. Additional amounts of CO_2 were introduced and further spectral data collected. For each of these data points, the composition of the ammonia compounds present was determined using the OLI software. The measured height of each peak was then matched with the predicted concentration, and a correlation curve developed allowing concentration of a species to be determined from peak height. Good agreement was achieved between measured and predicted values.

The tests were repeated but using 20-mole percent ammonia solution. Figure 17 shows the values predicted by the OLI software compared with values predicted from the Raman peaks using the calibration curve developed from the 14-mole percent ammonia solution. Agreement between the two sets of data was not good, and comparisons of ammonium carbamate and carbonate were similarly poor. More testing and analysis is required to understand how to achieve a correlation that is applicable to all concentrations of ammonia. The incentive for resolving this issue is that the Raman probe with its rapid response could potentially be used to monitor and control a commercial process.

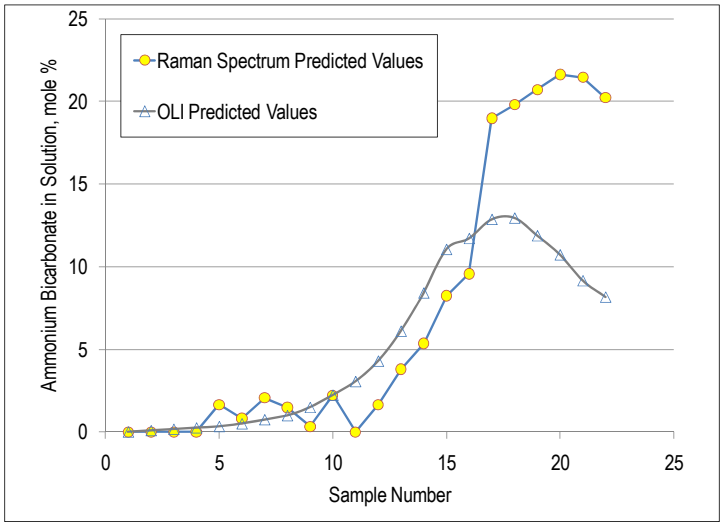

Figure 17. Comparison of Predicted Values for Ammonia Solution.

3.3.2 POLYDIMETHYLSILOXANE

Staff completed evaluation of a new solvent, polydimethyl siloxane (PDMS), which was tested at the recommendation of the DOE. The recommendation of PDMS was based on encouraging results obtained in a DOE-sponsored study at the University of Pittsburgh ("CO_2-Philic Oligomers as Alternatives for PEGDME in CO_2 Absorption"). In the study, the PDMS was compared to dimethyl ether of polyethylene glycol (DEPG) and several other oligomeric (consisting of up to five monomers) solvents. The PDMS was identified as one of the two best solvents studied in terms of immiscibility with water, CO_2 capture selectivity, and low viscosity. As DEPG is highly miscible with water, commercial processes must control water buildup, which imposes an energy penalty that could be avoided by the use of a solvent immiscible with water. For example, when DEPG is thermally regenerated to release H_2S, any water present is evaporated, thereby increasing the heat of regeneration.

The PDMS solvent was compared to DEPG in both off-line and on-line tests in the batch reactor in the SCU. The specific gravities and the mean molecular weights of the two solvents are listed in Table 12.

Table 12. Properties of PDMS and DEPG Solvents.

	PDMS	DEPG
Specific Gravity	0.87	0.99
Mean Molecular Weight, g/mol	515	280

In July 2010, four sets of tests were conducted off-line using bottle gases to begin exploring the CO_2 capture characteristics of PDMS and DEPG solvents. Initial tests were carried out at 20 and 40°C (68 and 104°F) to define the appropriate conditions for absorption and regeneration testing. Flash regeneration was demonstrated for both solvents with no evidence of foaming. As both the PDMS and DEPG are physical solvents, CO_2 capture efficiency and capacity is strongly influenced by the CO_2 partial pressure. The results formed the basis for further testing, also with bottle gases, completed under the operating conditions listed in Table 13.

Table 13. Nominal Test Conditions for Off-Line CO_2 Capture Testing with PDMS and DEPG.

Test Parameter	Nominal Values
Reactor Pressure, psia	155 to 330
Reactor Temperature, °F	70 and 100
CO_2 Concentration, vol%	20 and 40
CO_2 Partial Pressure, psia	30 to 130
Nitrogen Flow Rate, lb/hr	5.0
CO_2 Flow Rate, lb/hr	2.2 and 5.7

Further tests were completed on-line during R05 to investigate the absorption and regeneration performance of the PDMS and DEPG solvents. Testing consisted of a series of absorption-regeneration cycles. Absorption was carried out at 140°F and 175 psia. Regeneration was achieved either by lowering the pressure into the range 15 to 88 psia to flash off the absorbed species, or by increasing the temperature up to 300°F to release them thermally.

Figure 18 presents data for DEPG and PDMS showing the variation with time of the CO_2 concentration in the gas stream exiting the reactor during absorption cycles. The initial cycle was completed with fresh solution, which was flash regenerated by lowering pressure to near atmospheric. The minimum CO_2 attained in subsequent absorption cycles was not as low as for the initial cycle, indicating that flashing does not release all the CO_2 absorbed in the previous cycle. The minima showed that DEPG achieved higher absorption efficiencies than PDMS for the initial and subsequent cycles. Also, the CO_2 concentration profile indicated that absorption was maintained for a longer period, allowing DEPG to achieve a higher CO_2 loading level—approximately 1.4 times higher than PDMS based on the area within the concentration profiles.

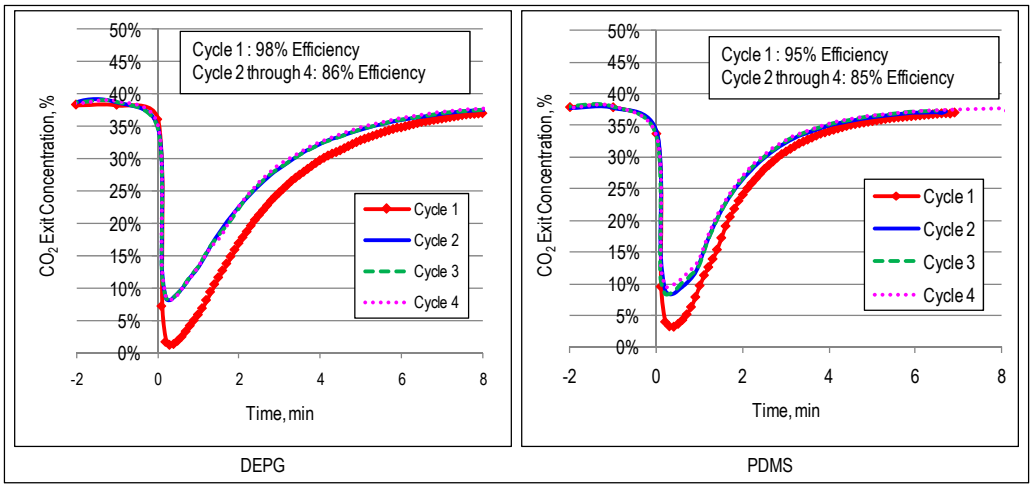

Figure 18. CO_2 Concentration Profile during Absorption Following Flash Regeneration.

Figure 19 presents the maximum CO_2 absorption efficiency as a function of the flash pressure used to regenerate the solvent prior to absorption. As flash pressure increased, less CO_2 was released and, as a consequence of the reduced free capacity, CO_2 absorption efficiency fell. Above 40 psia flash pressure, the PDMS appeared to release more CO_2, resulting in higher CO_2 absorption efficiency than for DEPG. At flash pressures below 40 psia, the differences between the DEPG and PDMS were less significant.

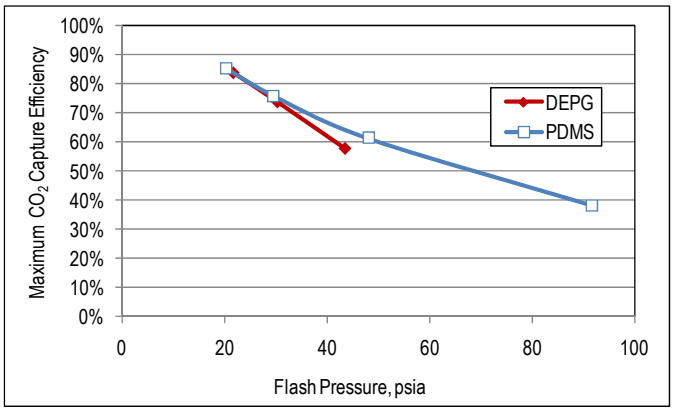

Figure 19. Effectiveness of CO_2 Regeneration at Different Flash Pressures.

Figure 20 presents data for the two solvents showing the variation with time of the H_2S concentration in the exiting gas stream during absorption cycles following flash regeneration. Measurement was provided by a batch gas chromatograph that gives a value every three minutes. This accounts for the appearance that the tests start before time zero. The gas sampling sequence was initiated to take a sample around one minute into the run to coincide with the minima identified by CO_2 test results. As for the CO_2 testing, the initial cycle was completed with fresh solution, which was flash regenerated by lowering pressure to near atmospheric.

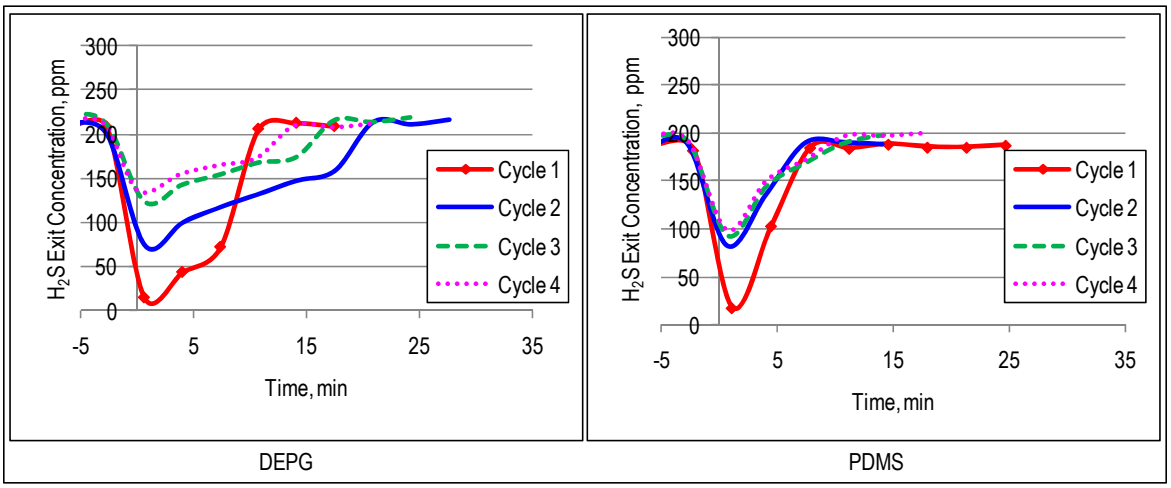

Figure 20. H_2S Concentration Profile during Absorption Following Flash Regeneration.

The minimum concentration during the initial absorption cycle was lower for the DEPG than for the PDMS, at 5 and 15 ppmv, respectively. Following the first flash regeneration cycle, the DEPG absorption minimum was still lower—75 ppmv compared to 85 ppmv for PDMS—indicating that the first flash stage was more effective at releasing the H_2S from DEPG. There was some departure from this trend for Cycles 3 and 4 with the DEPG minima values decreasing, indicating that these flash stages were less effective than the first one. The results indicate that DEPG continued to absorb H_2S and that the sites used later in the test sequence were less amenable to flash regeneration. In contrast, the trends for Cycles 3 and 4 for PDMS were almost the same as for the second cycle, indicating that saturation was reached more rapidly than for DEPG.

Figure 21 plots data for the two solvents showing the variation with time of the H_2S concentration in the exiting gas stream during absorption cycles following thermal regeneration at 150°C. The results show similar H_2S absorption efficiencies for the three cycles indicating that thermal regeneration released all the H_2S from both solvents. The H_2S concentration profiles indicate that absorption was maintained for a longer period with DEPG than with PDMS. From the area within the concentration profiles, the H_2S loading for DEPG is approximately 3.5 times higher than that for PDMS.

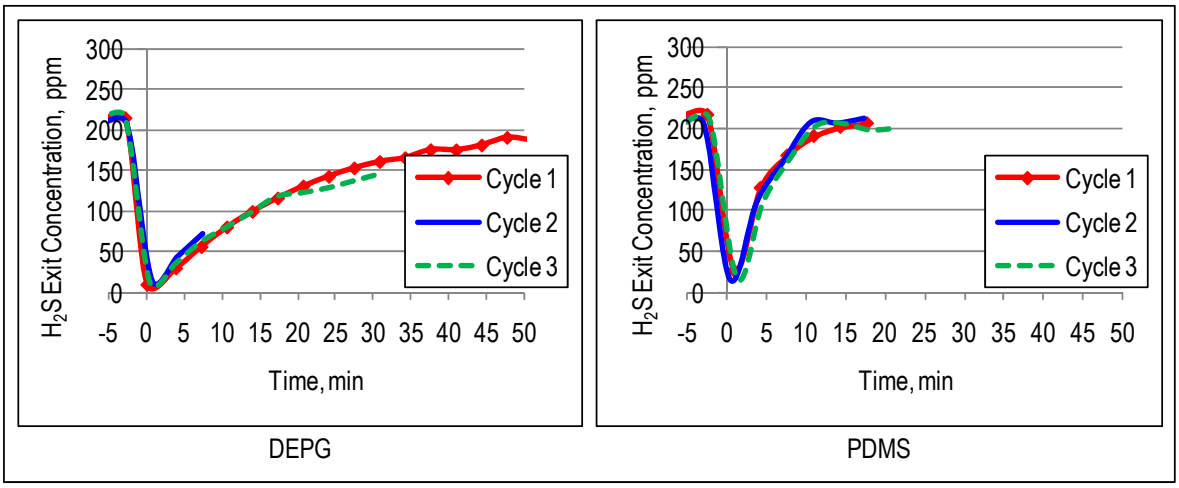

Figure 21. H_2S concentration Profile during Absorption Following Thermal Regeneration.

Figure 22 presents the maximum H_2S absorption efficiency as function of the flash pressure used to regenerate the solvent prior to absorption. As flash pressure increased, less H_2S was released, and as a consequence of the reduced free capacity, H_2S absorption efficiency fell. The trend of the data is similar to that of CO_2 presented in Figure 19, but the efficacy of H_2S flash regeneration was lower as indicated by the lower capture efficiency values achieved with H_2S.

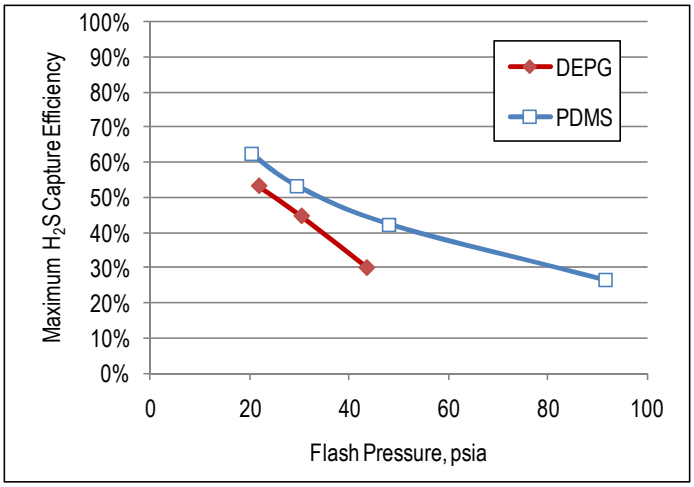

Figure 22. Effectiveness of H_2S Regeneration at Various Flash Pressures.

As DEPG has a high affinity for water, some of the regeneration energy required to release H_2S and CO_2 is used to evaporate water and stabilize the solvent moisture content. Since PDMS is immiscible with water, the water can be separated mechanically, eliminating evaporation duty and lowering the heat of regeneration. Ten weight-percent water was added to the solvents to determine the effect of water on CO_2 absorption and regeneration performance. The volume of solvent/water mixture added to the reactor was 4.6 liters to maintain the depth at 10 inches.

Figure 23 presents the moles of CO_2 absorbed in the mixtures. The amount absorbed by the DEPG-water mixture was lower than for DEPG only. The reduction was in the range 15 to

25 percent, more than the straight 10 percent through dilution with water. In contrast, the amount of CO_2 absorbed by the PDMS-water mixture is 5 to 15 percent higher than for PDMS only. With or without water addition, DEPG absorbs more CO_2 than PDMS.

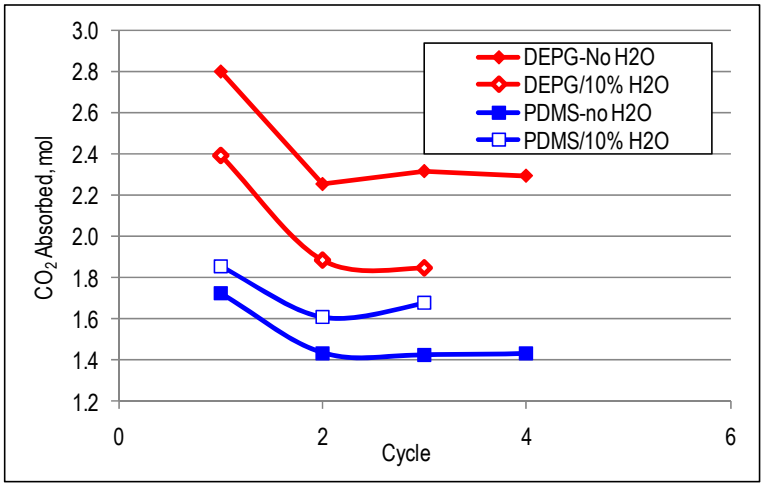

Figure 23. Effect of Water Addition to DEPG and PDMS on CO_2 Absorption.

3.3.3 POTASSIUM CARBONATE AND POTASSIUM PROLINATE

To widen the range of chemical solvents under investigation, potassium carbonate and potassium prolinate were tested in the batch reactor. Potassium carbonate is an established solvent and is used in the Benfield process for acid gas purification, and amino acids such as proline, are being investigated for post-combustion CO_2 capture. Properties of the solvents used are listed in Table 14.

Table 14. Properties of Potassium Carbonate and Potassium Prolinate Solvents.

	Molecular Weight, lb/lb-mol	Concentration		Absorption Temperature, °F
		mol%	wt%	
Potassium Carbonate	138	1.7	20	212
Potassium Prolinate	153	5.1	56	102

Potassium carbonate captures CO_2 forming a bicarbonate:

$$K_2CO_3 + CO_2 + H_2O \rightarrow 2KHCO_3 \quad \text{Equation 6}$$

Heat of reaction	-6.07 kcal/g mol	(249 Btu/lb CO_2)
Heat of crystallization	-9.64 kcal/g mol	(-395 Btu/lb CO_2)
Total	-15.71 kcal/g mol	(-644 Btu/lb CO_2)

The comparable values for ammonium carbamate/bicarbonate are (-521, -277, and -798 Btu/lb CO_2) so the potassium carbonate has lower heats of reaction. This advantage is offset by a lower rate of reaction requiring absorption at a higher temperature (212°F compared to 98°F) for ammonium hydroxide. Additionally, as $KHCO_3$ has a higher molecular weight, the CO_2 loading

is lower than that of ABC. To keep the K_2CO_3 in solution, the concentration is limited to 20 weight-percent. Together, these characteristics mean that the solvent flow rate is higher, increasing the heat of regeneration.

Amino acids have several advantageous properties such as low volatility and corrosivity, which offer advantages over amines. Research at the University of Twente in the Netherlands investigating amino acids for post combustion CO_2 capture concluded that L-proline had the highest reaction rate of the amino acid salts in one-molar aqueous solutions.

Tests were carried out at the NCCC using five-molar solutions to increase the CO_2 loading. Initial tests were carried out with the sodium salt formed by mixing the proline with sodium hydroxide. CO_2 was bubbled through the solution and very fine crystals were formed, eventually producing a thick mixture. Similar tests were completed with the potassium salt (using potassium hydroxide), but the final mixture was less viscous presumably because the potassium salt was more soluble.

Figure 24 compares the CO_2 capture efficiency for the three solvents presented on a molar basis as well as on a mass basis. The performance of the ammonia and potassium carbonate were similar, with the capture efficiency of potassium prolinate falling precipitously after exceeding a molar ratio of 0.5. The CO_2 mass loading for ammonia was shown to be greatly in excess of the other two solvents, with the potassium carbonate having the lowest loading.

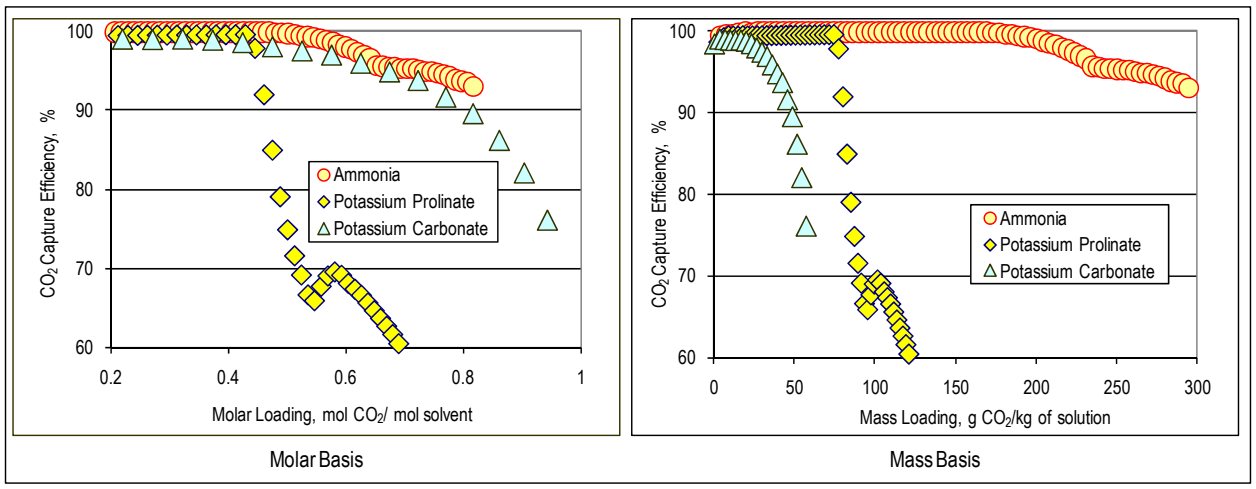

Figure 24. CO_2 Capture Efficiencies for Potassium Prolinate and Potassium Carbonate.

Figure 25 graphs the pressure rise in the reactor during heating for each of the three solvents. No CO_2 was vented from the reactor, so all the CO_2 released resulted in pressure increases. The factor "L" represents the molar loading of CO_2, that is, moles of CO_2 per mole of solvent. The higher pressure indicates that the ammonia solution released CO_2 more readily and was regenerated more fully than the two other solutions.

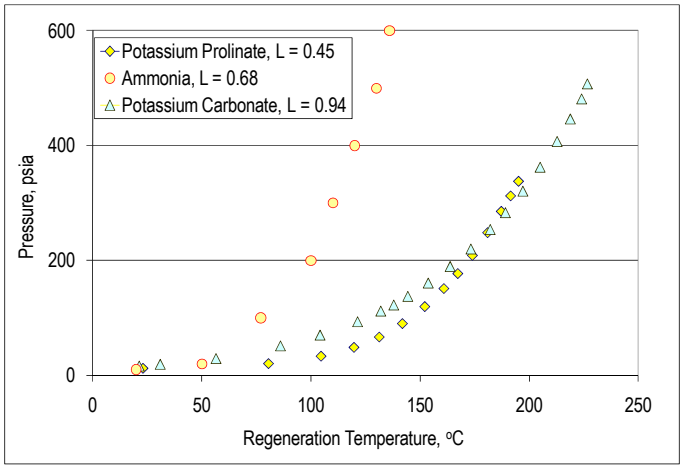

Figure 25. Pressure Increase during Regeneration of Three CO_2 Capture Solvents.

3.4 GAS SEPARATION MEMBRANES

During BP2, the NCCC continued its support of gas membrane testing, which has been ongoing for several years. A portion of the SCU was made available to MTR and to MPT for testing of membrane technologies.

3.4.1 MEMBRANE TECHNOLOGY & RESEARCH HYDROGEN AND CO_2 MEMBRANES

MTR is a private company in Menlo Park, California, which designs, manufactures, and sells polymeric gas-separation membranes for petrochemical and natural gas applications. Since 2007, the company has been carrying out R&D in CO_2 separation from coal-derived flue gas and syngas.

Figure 26 provides a cross-sectional view of MTR's thin-film composite membrane structure. The micro-porous support membrane provides the mechanical strength required and is coated with a 0.5- to 1.0-micron thick gutter layer that provides a smooth surface on which to coat the selective membrane layer, which is about 0.05 to 0.1 micron thick. A surface coating on the selective layer protects it from mechanical damage. The gutter layer and surface coating are sufficiently permeable to allow the permeating gases to pass through readily.

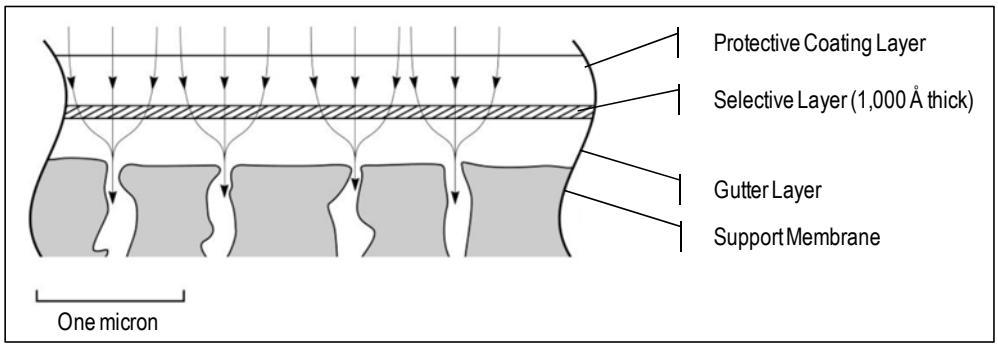

Figure 26. Schematic of MTR's Thin-Film Composite Membrane.

MTR uses a spiral-wound configuration for membrane production, which is shown in Figure 27. A sheet of thin-film composite membrane is cut to the required length and folded in half to create an envelope. Spacer material (the permeate spacer) is placed between the two surfaces to create a flow channel for the permeate stream, and the two parallel edges of the envelope are glued together. The remaining open edge is secured to a perforated collection tube and spacer material (the feed spacer) is placed over the membrane surface. Additional membrane envelope sections with feeder spacers are secured to the collection tube in a similar manner until the specified membrane area is reached. The membrane envelopes and feed spacers are then wrapped around the tube, and the module is inserted into a steel pipe.

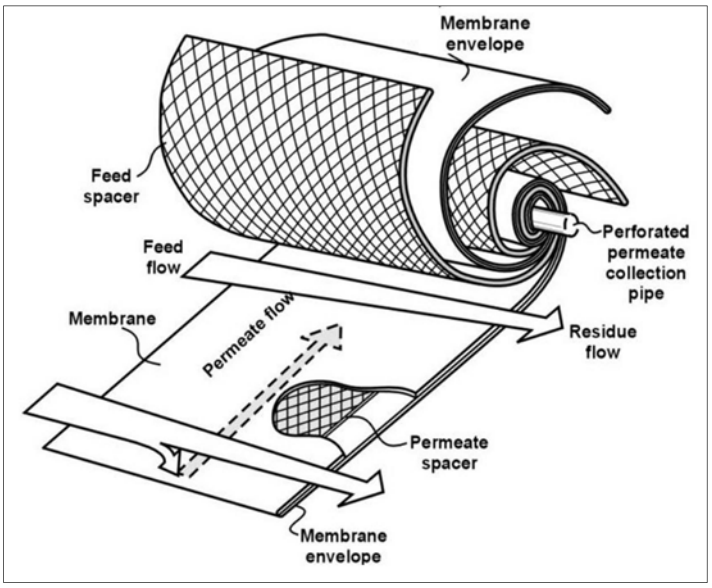

Figure 27. Schematic of MTR's Spiral-Wound Membrane Assembly.

The feed gas is fed to one end of the pipe and enters the feed spacer channels of the membrane module. The permeable gases pass through the membrane layer and flow along the permeate spacer channel toward the central collection pipe and exit the membrane module at low pressure. The residual gases that do not permeate through the membrane continue to flow along the feed spacer channel and exit the membrane module and the pipe section at high pressure.

In November 2009, MTR began testing two polymeric membranes at the NCCC to process coal-derived syngas, one a CO_2-selective Polaris™ membrane and the other a H_2-selective Proteus™ membrane. The prototype CO_2 membrane assembly is approximately 3-feet long with a 4-inch outer diameter (OD) and is installed in a skid-mounted tube able to accept two modules. The H_2 membrane is flat sheet installed in a 6-inch diameter, high-pressure permeation cell set in a small pressure vessel. Figure 28 provides photographs of the membrane mounting equipment.

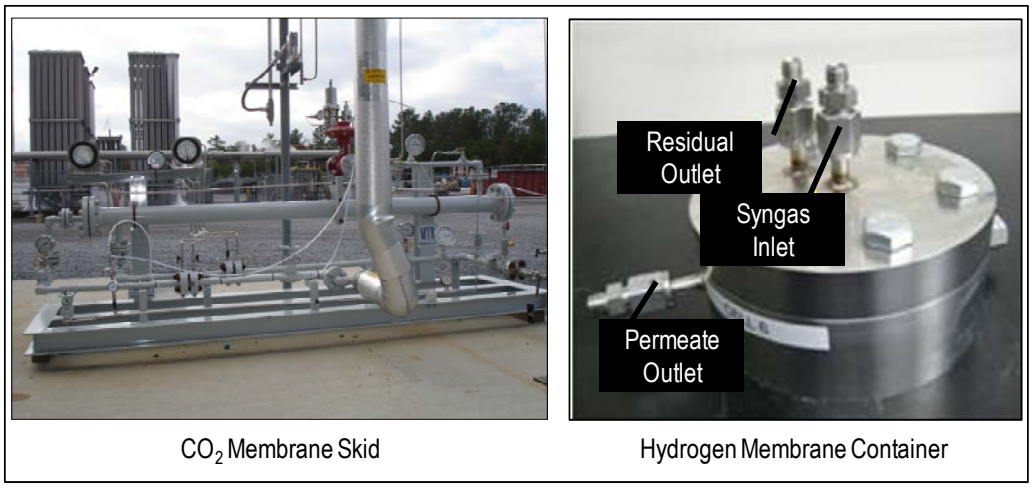

Figure 28. MTR Membrane Test Equipment.

High-temperature syngas from the SCU is cooled by bubbling through a water bath that also removes the small amount of hydrocarbons present. The permeate and residual streams leaving the membranes are analyzed, then re-combined and returned to the exit syngas header.

Table 15 summarizes the conditions for membrane testing during gasification test runs R03, R04, and R05. In R03 and R04, the CO_2 membrane operating temperature varied with ambient conditions, and for R05, the membrane tube was heat traced and insulated to maintain steady operating temperatures.

Table 15. MTR Membrane Test Conditions.

Test Parameter	Test Run R03	Test Run R04	Test Run R05
Syngas Conditions	Unshifted, sweet	Shifted, sour	Shifted, sour
Coal	PRB	Lignite	PRB
Membrane Temperature, °F (CO_2/H_2)	49/250	68/250	82/250
Membrane Surface Area, m^2 (CO_2/H_2)	0.8/30	3.2/30	3.2/30
Membrane Pressure, psia	150	190	190
Hours of Operation	500	500	800
Syngas Flow Rate, lb/h (CO_2/H_2)	10/1	50/1	50/1
Mean Inlet Syngas Composition (Dry Basis)			
Hydrogen, vol%	9.3	12.5	13.6
CO_2, vol%	11.7	14.1	14.8
CO, vol%	5.7	2.2	2.8
H_2S, ppmv	Less than 10	780	360

Figure 29 plots the results of CO_2 membrane operation during R03, showing the variation with time for the permeance of gases in the syngas and the selectivity of CO_2 relative to these gases. The term “gpu” used in the mixed gas permeance plot in Figure 29 represents the gas permeation unit, which is the volumetric flow rate per unit cross sectional area for a given pressure differential in units of (10^{-6} standard cm^3) / (cm^2*s*cmHg).

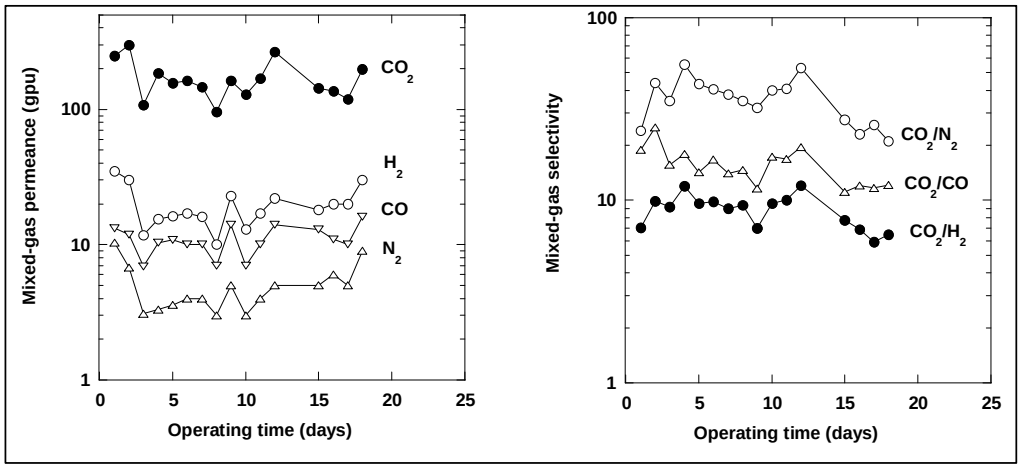

Figure 29. MTR CO_2 Membrane Performance during R03.

The CO_2 concentration in the permeate was 4 to 5 times that of the feed steam, and the H_2S concentration was about 6 times higher in the permeate than in the feed stream. During the testing, the membrane operated stably with the variations shown in Figure 29 occurring primarily from changes in ambient temperature, with a lesser effect of syngas composition and flow rate.

Figure 30 presents test results for the hydrogen membrane at two operating temperatures during R04. For a temperature increase from 120°C to 135°C, the hydrogen permeance increased from 190 to 270 gpu, and the H_2/CO_2 selectivity decreased from 24 to 17. Nevertheless, the membrane performance exceeded target values for these two parameters at both temperatures. Results from all three test series indicated that hydrogen in the feed stream was enriched 6 to 8 times in the permeate stream. The presence of H_2S in the syngas feed did not compromise membrane performance.

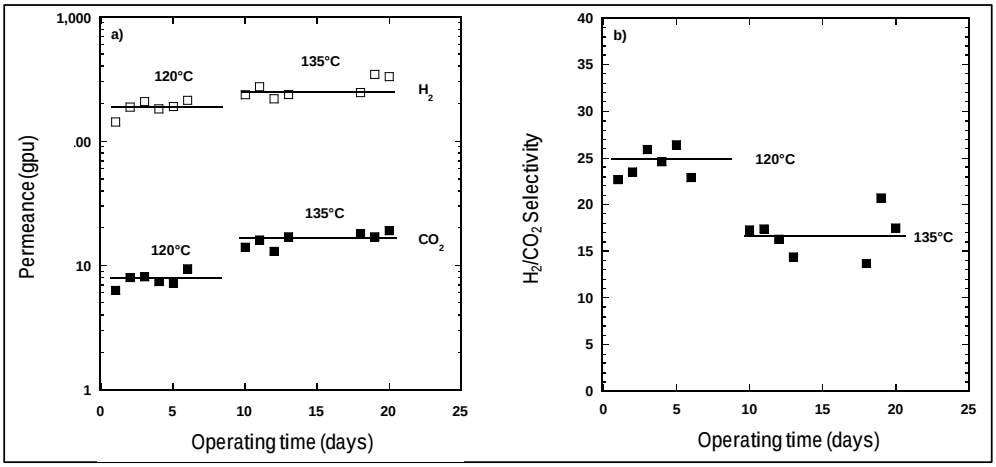

Figure 30. MTR H_2 Membrane Performance during R04.

For hydrogen membranes designed to separate 90 percent of the hydrogen from coal-derived syngas, the DOE has set a target of limiting the cost of electricity increase by more than

10 percent. The results of MTR's analysis for the hydrogen membrane, including test data from the NCCC, indicate that the increase in cost of electricity would be 15 percent, half that achieved using Selexol (according to MTR) but still above the DOE targeted value of 10 percent. Hence, some improvement in membrane performance is required, and the NCCC is expecting to support the testing required to achieve the necessary enhancement.

In summary, both the CO_2-selective Polaris membrane and H_2-selective Proteus membrane have performed well using coal-derived syngas. The results are consistent with those from MTR's bench-scale test using simulated syngas. Stable membrane performance under industrial conditions is encouraging for further development of polymeric membrane technology.

3.4.2 MEDIA & PROCESS TECHNOLOGY HYDROGEN MEMBRANE

The MPT Carbon Molecular Sieve hydrogen membrane was developed to demonstrate efficiency gain in the water-gas shift reaction while producing hydrogen from coal-derived syngas in a "one-box" configuration. The membrane was designed to enhance CO conversion in fuel gas via the removal of hydrogen in-situ, and/or yield high purity hydrogen as a product or co-product. The key feature of the one-box process is to limit pre-treatment requirements to particulate removal only. The membrane was first tested at the PSDF in 2008, which marked the first time a hydrogen-selective membrane was successfully operated on untreated coal-derived syngas.

The MPT membrane operating temperature ranges from 480 to 570°F. At the lower temperature, the permeability is low but the selectivity is high and vice versa for the higher temperature. Since the PSDF syngas is more diluted by nitrogen than would be syngas from a commercial facility, bottled hydrogen was added to the syngas for the membrane testing, increasing the hydrogen concentration from about 10 percent to 55 percent.

Testing was initially completed using a single-tube ceramic membrane 30 inches long with a 0.225-inch outer diameter housed in a 0.375-inch inner diameter stainless steel tube. For R04, MPT scaled up its single-tube membrane test unit to a multiple-tube assembly consisting of ten tubes similar to those in the single-tube arrangement. The tubes were housed in a 4-inch outer diameter stainless steel vessel using compression fittings with graphite ferrules to secure the tubes to the tube sheet. For this arrangement, the membrane material was coated on the outer tube surface to increase the membrane area per tube. The inlet syngas flow rate, augmented with hydrogen, was 12 lb/min with a maximum operating temperature of 450°F. While testing at this temperature, the permeate flux fell by 10 percent because of hydrocarbons condensing on the membrane surface.

The use of compression fittings proved cumbersome, so an improved design consisting of fourteen tubes held in position by fused glass in a ceramic collar was designed for testing in R05 (see Figure 31). The assembly was installed in a 2-inch outer diameter stainless steel tube. The inlet syngas flow rate, augmented with hydrogen, was 20 lb/min. At the 530°F operation temperature, the permeate flux remained constant, indicating that no hydrocarbon deposition had occurred. The modifications also improved controls and enabled continuous operation for over 100 hours.

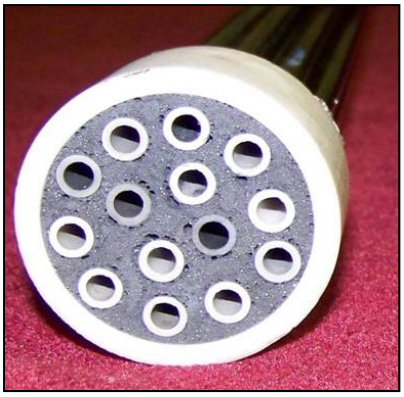

Figure 31. Media & Process Technology Hydrogen Membrane Assembly.

Table 16 shows pure gas permeation measurements made with nitrogen and helium following testing in run R05.

Table 16. Pure Gas Permeance Measurements of the MPT Hydrogen Membrane.

Temperature, °F	Permeance, $m^3/m^2/hr/bar$		Ideal Selectivity (He/N_2)
	N_2	He	
514	0.019	1.02	53
392	0.011	0.80	70
214	0.008	0.48	64

The measurements show that nitrogen and helium permeance increases substantially from 392 to 514°F but the selectivity (He/N_2) peaked at around 392°F. The temperature effect on selectivity explains the variation in permeate hydrogen content measured in the test program.

These results indicate that the MPT carbon molecular sieve membrane operating at 530°F can be used to separate hydrogen from raw syngas without any reduction in performance. This temperature is compatible with water gas shift catalytic reactor temperature indicating that the water-gas shift reaction and hydrogen separation could potential be incorporated into a single unit process.

The MPT membrane is still relatively small but testing at the NCCC along with the technical support provided, has assisted in increasing the size of the test modules and progressing the technology along the path to commercialization.

3.4.3 MEMBRANE MATERIAL COUPON TESTING

NETL selected a number of coupons of materials under consideration for use in hydrogen membranes to be exposed to coal-derived syngas at around 750°F. The materials were installed inside the hot gas filter vessel downstream of the filter elements. The data collected allows comparison of corrosion rates using actual coal-derived syngas with those collected in the laboratory using simulated syngas. The coupon types exposed were as follows:

- Materials from NETL Pittsburgh approximately 100 microns thick, including Pd, PdCu (5 samples), PdCuX (4 samples), PdX (7 samples), and 2 miscellaneous alloys
- Six supported membrane materials from Worchester Polytechnic Institute, which included composite Pd and PdCu on porous stainless steel
- Four structural alloy materials from NETL Albany

Each coupon was approximately one-inch square with a 0.125 inch diameter hole in one corner to allow the coupons to be wired inside a stainless steel mesh box in the filter vessel. The coupons were exposed to syngas for 1,000 hours at mean conditions of 750ºF, 7.5 vol% hydrogen, and 250 ppmv H_2S.

Analysis of the exposed coupons is still in progress. Analysis procedures being used include:

- Weight change
- X-ray diffraction
- Scanning electron microscopy (SEM) with energy dispersive spectroscopy of the exposed surfaces and prepared cross sections
- Elemental analysis using inductively-coupled plasma optical emission spectrometry and inductively-coupled plasma mass spectrometry

Some of the X-ray diffraction results are presented in Figure 32. These show that a membrane consisting of only palladium sulfides failed within 1,000 hours of exposure. The resistance to corrosion was increased as the percent of copper in the coupon material increased. However, based on previous membrane testing, increasing the copper content decreases the hydrogen permeability of the alloy.

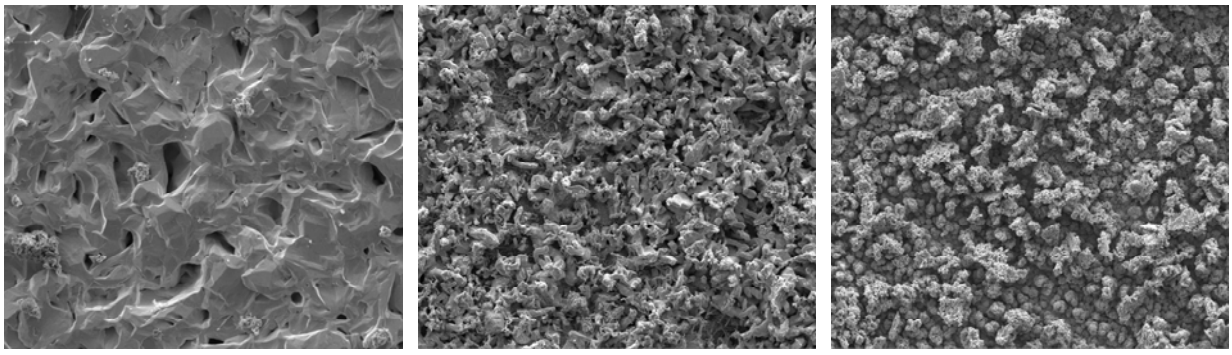

Pd only-- Only Pd_4S phase detected. Pd coupon completely sulfided and fractured.	80-wt% Pd in Cu-- Thick sulfided corrosion layer of $Pd_{13}Cu_3S$ with trace of Pd_4S detected. Pd metal not detected .	60-wt% Pd in Cu--Only ordered-body centered-cubic alloy detected. Sulfides visible by SEM are below detection limit of standard scan conditions used.

Figure 32. X-Ray Diffraction Analyses of Membrane Material Coupons Exposed to Filtered Syngas.

4.0 POST-COMBUSTION CO_2 CAPTURE

Design and construction of the PC4 continued at the Alabama Power E.C. Gaston plant site (see Figure 33). The layout of the PC4, shown in Figure 34, contains several areas for testing of carbon capture technologies, a control room building, electrical infrastructure, and a Balance of Plant (BOP) area containing utilities and chemical storage/handling. Fabrication of the PSTU, a major part of the PC4 test equipment, and utility bridge modules continued during BP2. Initial commissioning activities were underway during the last part of the year.

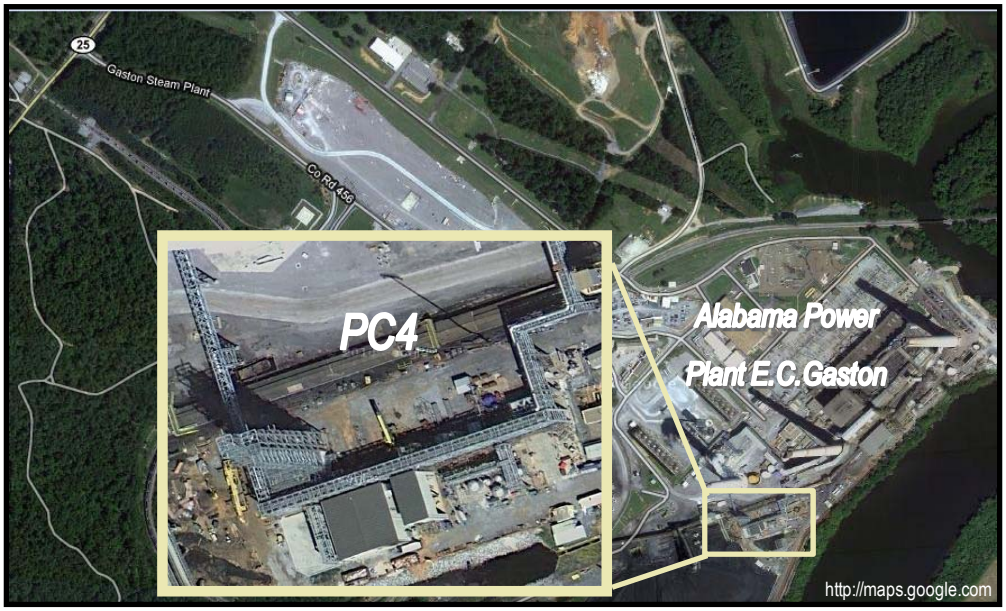

Figure 33. PC4 Site at the E.C.Gaston Plant.

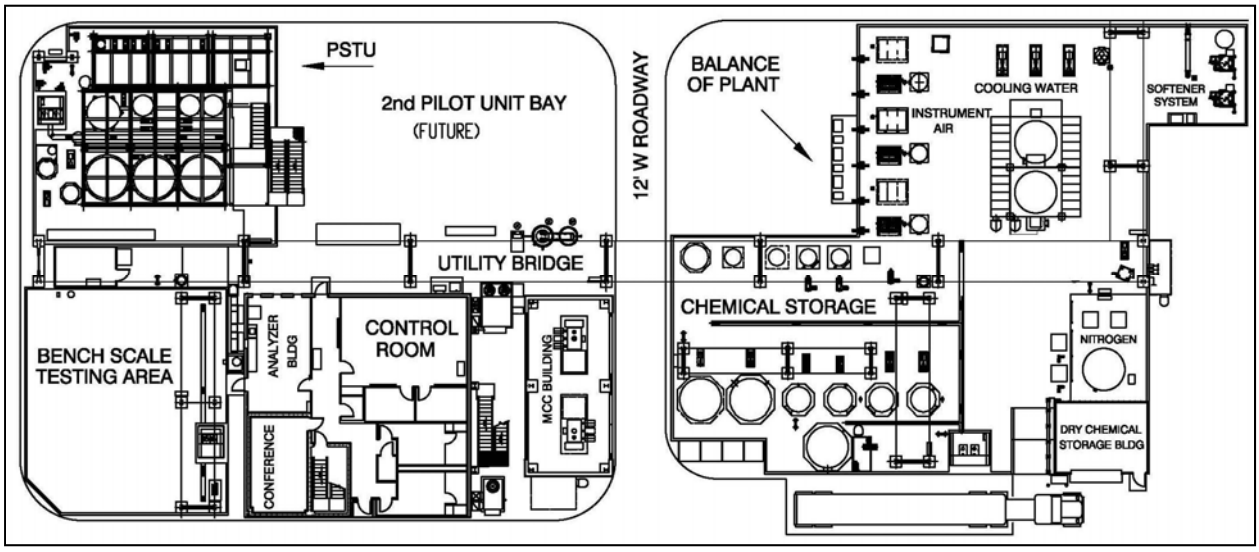

Figure 34. PC4 Site Layout.

4.1 PC4 DESIGN AND CONSTRUCTION

Site Preparation. At the end of Budget Period 1, the PC4 site preparation work concluded with recovery of an area from the Plant Gaston coal pile run-off pond, leveling and compaction of the site, and commencement of caisson installation. During the first quarter of BP2, installation of caissons was completed, with a total of 75 caissons and 30 micropiles installed to provide a solid base for continued installation of foundations and other civil engineering components. The micropiles were required in some areas where existing underground piping and electrical conduits could not be rerouted. In addition, 54 piers were installed at the top of the caissons in preparation of setting support columns for utility bridge modules. Figure 35 shows the site preparation work in progress.

Caisson and Pier Installation

Cooling Tower Piping Reroute

Figure 35. PC4 Site Preparation Work.

Construction of Foundations. Civil design and foundation installation was completed. Installation of foundations began near the end of the 1st quarter, beginning with the PSTU base slab and the motor control center (MCC) building and transformer foundations. Design and construction of the BOP and control room foundations were completed next, followed by the bench-scale testing area slab, which was completed early in the third quarter. Foundation work included excavation, forming, installation of rebar and embedded grounding/piping, and pouring and finishing of the concrete. The PSTU, bench scale testing area, and the BOP area required installation of sumps and trenches along with the curbed base slab fabrication. In addition, a chemically resistant coating was applied to all concrete surfaces. Space for a second pilot unit was reserved for future use.

Following completion of base slabs, design and installation of pads for storage tanks, pumps, compressors, heat exchangers and the cooling tower was completed. Figure 36 shows the chemical storage area pads.

Figure 36. BOP Area Foundation with Chemical Storage Tank and Pump Pads.

Utility Bridge. The utility bridge modular design was finalized with the fabricator early in the 1st quarter of BP2, after which the steel and piping fabrication began. Assembly of the utility bridge modules continued into the 2nd quarter, which entailed significant work in piping as well as heat tracing and insulation. The bridges were staged at the assembly site to insure proper fit when erected on the bridge columns installed during the site preparation phase earlier in the year.

The first utility bride modules were delivered and installed in May, with all but four of the remaining modules delivered and installed in June. Installation of the last four modules, installed over a roadway, had to be scheduled after the PSTU assembly was completed, because the roadway was needed for disassembly of the large crane used for PSTU assembly. Figure 37 shows installation of bridge modules.

Figure 37. Installation of PC4 Utility Bridge.

Control Room/Administration Building. Turnkey fabrication of the control room/administration building was awarded in the 1st quarter of BP2. The building layout and details of the vendor design were reviewed and finalized with the vendor. In addition, design for all in-slab plumbing, grounding, and drains was completed, and these were installed. The heating, ventilation, and air conditioning system design was also completed. After installation of the foundation, construction of the building began, with fabrication completed in the 3rd quarter.

Motor Control Center Building. Civil and architectural design of the MCC building was completed early in the 2nd quarter, during which the foundation for the building was completed. Construction of the building was completed in the 3rd quarter. Work the remainder of the year included installation of cable trays, power distribution, switchgear grounding, and lighting panels. In addition, installation and termination of wiring in the programmable logic controller (PLC) panels was completed.

Pilot Solvent Test Unit. At the end of BP1, the PSTU process design had been completed, and an award had been made for supply of a modularized test unit. In addition, detail design, procurement, and off-site fabrication of the PSTU modules had begun. During the 1st quarter, fabrication of the packed bed columns and other equipment was completed, and assembly of the modules began at the fabrication site. Assembly included installation of packing in the columns.

During the 2nd quarter, procurement of PSTU materials and equipment was completed, the modular construction was completed, and the modules were fully assembled. Shipment of the modules to the PC4 site began at the end of the 2nd quarter, and assembly of the modules was completed by the end of July. After assembly, structural interconnections of the PSTU modules were completed, grating and handrails required to access the PSTU were installed, and mechanical and electrical interconnections between the modules were completed. Figure 38 shows the PSTU after installation.

Figure 38. Installed PSTU Structure.

After assembly of the PSTU and utility bridge, interconnections of piping and wiring between modules began and continued for the remainder of BP2. Part of this scope included fiberglass reinforced plastic (FRP) interconnections between modules and vessels.

Mechanical Engineering Design. Major equipment 3-D modeling was completed in the 1st quarter. Layout drawings were prepared throughout the year for civil detail design and construction activities. The PSTU design also included development of a 3-D model, which greatly assisted

field personnel during fabrication. Figure 39 compares a model snapshot with actual field construction.

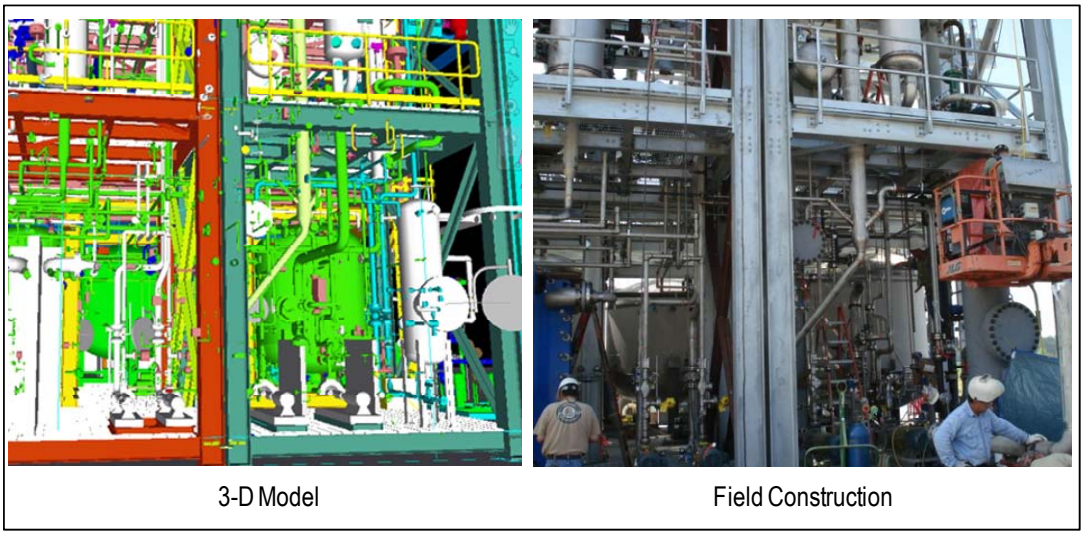

Figure 39. PSTU 3-D Model and Construction.

General BOP area layout drawings and mechanical arrangement drawings were prepared and issued for a number of areas. Under-slab drain drawings were prepared and issued for all process and building foundations. A significant number of isometric drawings were developed and issued—approximately 375 drawings for the PSTU, 400 for the utility bridge, and 300 for the BOP areas. In addition, several iterations of P&IDs were completed and issued throughout the year. As construction progressed throughout the year, mechanical design staff checked piping between equipment and connections to the utility bridge, provided field installation support, and developed and issued as-build drawings.

Equipment procurement continued early in the budget period. Specifications were developed for additional equipment and inquiry packages issued for quotes. Bids were reviewed, submittal drawings reviewed and purchase orders placed for a condensate cooler, water softener, various chemical metering pumps, potable water booster pumps, sanitary lift station, and eyewash and safety showers. Bulk materials (pipe, valves, and fittings) were ordered for the BOP areas. BOP equipment such as the cooling tower, instrument air compressor, tanks, and pumps were received during the first half of the year.

Vendor fabrication and assembly continued for 18 solvent and water pumps for the BOP solvent storage, cooling tower, process area sumps and various water supply systems (condensate, demineralized water, and process water). Early in the 1st quarter, vendor drawings for the 11 chemical storage tanks were reviewed and approved, and fabrication of the tanks began. Quality assurance visits were made to vendor shops as work progressed.

Electrical Engineering Design. Electrical design progressed throughout the year. The two 2,500 KVA transformers for supplying power to the site were purchased. Specifications were

completed and purchase orders issued for the MCC cable bus and 480 volt switchgear, and an inquiry package was issued for the BOP MCC. Electrical design activities also required significant work in the areas of power wiring, lighting design, process and freeze protection heat tracing, and lightning protection. Detailed drawings that were developed included power and lighting plans, heat tracing drawings, auxiliary system drawings, and site grounding grid and foundation grounding embed drawings. Approximately 1,100 electrical drawings were developed and issued to construction.

Instrumentation and Controls Engineering Design. Design, specification, and purchasing of instrumentation were completed. Approximately 300 instruments were provided for the PSTU and approximately 250 instruments for the BOP areas. Other instrument and controls design activities included development of loop sheets and instrument specification sheets, PLC panel drawings, instrument interconnection diagrams, and instrument installation detail drawings. Approximately 735 total instrument drawings were developed.

Bids were received and reviewed for six PLC electrical panels, and a purchase order was issued. After the vendor completed fabrication of the panels, they were shop tested, delivered to the site and successfully installed and commissioned. Design and procurement was completed for distributed control system cabinets to enable communication of PC4 instruments with the E.C. Gaston plant control system related to utilities supplied from the E.C. Gaston plant. Configuration of all PSTU and BOP PLCs was completed, including human-machine interface (HMI) configuration development. Configuration was completed for approximately 300 PSTU instrument points and 275 BOP points. Also, approximately 100 graphic screens were developed for the PSTU and BOP areas combined. Network server computers were specified, purchased, installed, and commissioned.

Balance of Plant Installation. A critical milestone early in BP2 was completion of tie-in connections to the E.C. Gaston Unit 5 utility systems that had to be made during a plant outage in February. These tie-ins involved the flue gas supply, flue gas return, firewater, and steam supply systems and taps upstream of the scrubber. In addition, 4,160-volt cable was pulled and tied into the switchgear installed during a previous outage, and control wires between the switchgear and control room were pulled and terminated. Additional utility tie-ins were completed during the year.

All equipment in the BOP area was installed, and installation of piping, electrical and instrumentation was completed in support of the hydrodynamic commissioning activities described in Section 4.2.2. All base utility supply systems were completed (cooling water, instrument air, filtered water, and potable water). All BOP storage tanks and pumps were set in place, and piping interconnections between tanks, pumps, and the utility bridge were installed. The steam supply header from E.C. Gaston to the PC4 site was completed through the power plant up to the PC4 battery limits. Installation of the flue gas supply header was completed. Other BOP systems completed included water supply pumps and piping and safety shower distribution.

4.2 PILOT SOLVENT TEST UNIT

The PSTU is designed to achieve 90-percent CO_2 capture using a 30-percent aqueous monoethanolamine (MEA) solution. This is the reference solvent to determine base line performance against which other solvents tested will be compared. These solvents may include hindered amines, amino acid salts, and ionic liquids. To accommodate the range of solvent properties, the PSTU design is very flexible operationally. A schematic of the PSTU is presented in Figure 40. Major design features are listed below.

- The vessels are spaced to allow for modifications and additional equipment to be installed to investigate alternative flow schemes.
- The regenerator is designed to operate at up to 215 psia as some solvents can be regenerated at pressure offering the advantage of a reduced CO_2 compression ratio.
- The absorber and regenerator are designed to allow alternative packing and other gas-liquid contacting arrangements to be readily installed.
- The absorber and regenerator are designed with numerous process nozzles to allow for different flow schemes and with sufficient instrumentation nozzles for comprehensive data collection.
- The system is designed to cover a wide range of flue gas and solvent flow turndown to accommodate process variations arising from the use of solvents with different properties. The turndown ratios are 2:1 for gas and from 3:1 to 5:1 for liquid.
- As a range of solvents is to be used, the equipment is easily drained and cleaned.
- As the corrosivity of the different solvents is not known, for experimental convenience the vessels are made from 316L stainless steel.

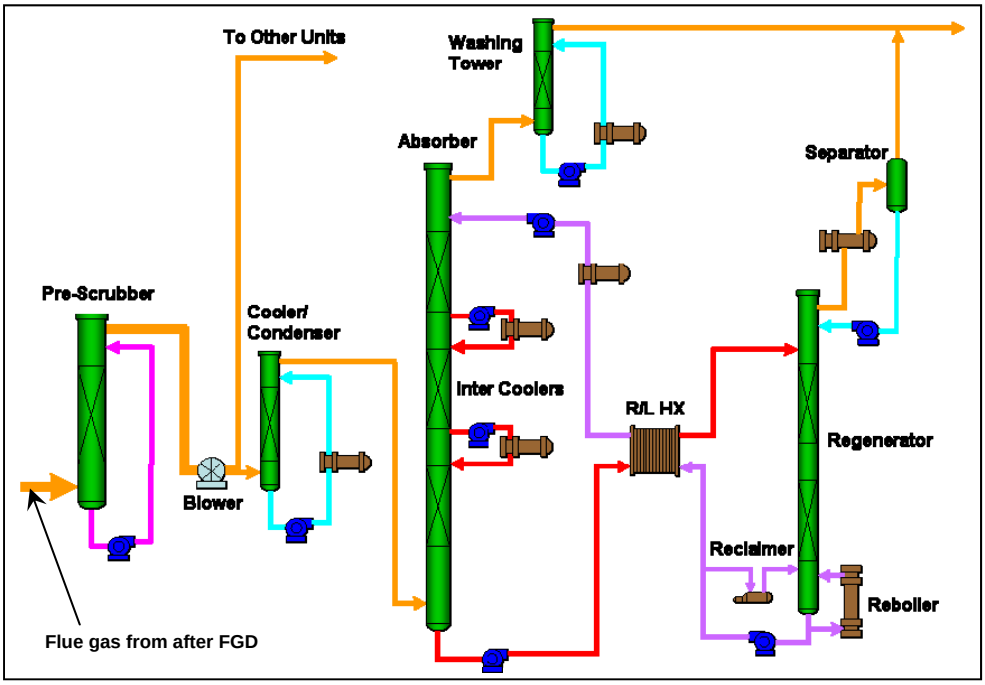

Figure 40. Schematic of PSTU.

Up to 35,000 lb/hr of flue gas is extracted from downstream of the FGD and passed to PC4 to support testing activities. Of this amount, 5,000 lb/hr flows to the PSTU. There are five major columns, or sub systems (shown in green in Figure 40), and their function will be discussed individually. Table 17 lists selected properties of the columns.

Table 17. Design Characteristics of PSTU Columns.

Column	Height, ft	Outer Diameter, inches	Number of Beds	Packing type
Pre-Scrubber	46	30	1	Random
Cooler/Condenser	30	24	1	Structured
Absorber	108	26	3*	Structured
Washing Tower	30	24	1	Structured
Regenerator	75	24	2*	Structured

*with additional capacity

Pre-Scrubber. This sub-system removes the small amount of SO_2 remaining in the flue gas after the treatment in the FGD. It is designed to handle up to 12,000 lb/hr, the additional amount being used to provide desulfurized flue gas to other test units.

Flue gas in a 14-inch FRP pipe enters at the bottom of the pre-scrubber and flows upward counter-currently to the 5-weight percent caustic soda solution used to remove the SO_2. The caustic soda solution is circulated through a tank operating in batch mode. Periodically liquid is removed to control the sulfate content and fresh caustic soda is added. The liquid removed is sent to the PC4 BOP for treatment. The treated flue gas leaves from the head of the vessel, being drawn through by a blower that also drives the flue gas through the cooler/condenser. The blower generates a head of 2.5 psi.

Cooler/Condenser. This sub-system cools the flue gas to an appropriate temperature for the CO_2 absorption reaction. Cooling also lowers the flue gas water content and limits dilution to the solvent solution in the absorber.

Absorber. This sub-system promotes efficient gas-liquid contacting to remove CO_2 from the flue gas. Flue gas in a 10-inch FRP pipe enters at the bottom of the absorber and flows upwards counter-currently to the CO_2-lean solvent returning from the regenerator. The CO_2-rich solvent leaves at the foot of the absorber and passes to the regenerator. The CO_2-depleted flue gas leaves from the head of the vessel and passes to the washing tower.

The absorber contains three sections in which packing is installed, and a fourth section can be added if required. The absorption reaction is exothermic and will raise the temperature of the solvent. If it rises too much it will limit the rate of CO_2 absorption and reduce the capture efficiency. An inter-cooling loop between adjacent sections of packing provides solvent temperature control.

The cool-rich solvent is pumped from the foot of the absorber to a cross-flow heat exchanger that recovers heat from the hot-lean solvent pumped from the foot of the regenerator. The cool-lean

solvent passes to the top of the absorber but can also be introduced at different levels in the absorber as part of the investigation to optimize CO_2 capture efficiency. The hot-rich solvent passes to the top of the regenerator. Before doing so the hot-rich solvent can be passed to a vessel in which some of the CO_2 is flashed off, thereby lowering the duty of the regenerator reboiler.

Washing Tower. This sub-system cools the CO_2-depleted flue gas removing trace amounts of entrained solvent and lowering the moisture content of the exiting gas, thereby reducing solvent make-up water requirements. The flue gas leaves the washing tower and flows to the inlet of the FGD.

Regenerator. The regenerator provides the heat required to release the CO_2 from the solvent. The hot-rich solvent (with or without flashing) flows down the regenerator through the packing or trays, coming into contact with steam rising from the reboiler. The resulting increase in temperature releases the CO_2 from the solvent. Part of the hot-lean solvent leaving the bottom of the regenerator passes to the reboiler to be heated and raise the inlet regenerating steam. The remaining solvent passes to the cross-flow heat exchanger to transfer its heat to the cool-rich solvent leaving the absorber. The reboiler heat source is low-pressure steam.

Intermittently, a small stream (about 4 percent) of the hot-lean solvent is treated to remove heat stable salts that form through reaction of the solvent with oxygen and SO_2. The stream passes to a reclaimer where caustic soda is added to degrade the salts and release the solvent. The mixture is heated, and the solvent and water vapor are returned to the foot of the regenerator, leaving the salts in the reclaimer.

The CO_2 exiting the regenerator (and any from the separator) is cooled to recover solvent and water vapor. The CO_2 flows to the inlet of the FGD, and the condensate flows to the regenerator.

4.2.1 PSTU TEST PLANNING

The measurement techniques and instrument locations were selected to ensure accurate measurement of the following:

- Flue gas and solvent flow rates
- Flue gas temperature and pressure
- CO_2 concentration in gas streams
- CO_2 loading in solvents
- Steam and cooling water flow rates
- Steam conditions
- Emissions performance
- Contaminants/degradation products
- Corrosion rates

The objective is to achieve accurate heat and mass balances to ensure valid determination of these parameters:

- Solvent performance characteristics
- CO_2 capture efficiency
- Regeneration energy requirements
- Absorber contact efficiency
- Environmental performance

Test Conditions. Prior use of amine solvents indicates that the major parameters affecting CO_2 capture are the liquid-to-gas ratio (L/G) in the absorber and the steam-to-liquid ratio (S/L) in the regenerator. Increasing S/L releases more CO_2 from the rich solvent so that the lean solvent returning to the absorber has a lower CO_2 content. This increases the CO_2 driving force in the absorber, increasing the amount of CO_2 captured. To maintain the same percent capture, the L/G ratio would be reduced. The most cost-effective operating condition would be determined from analysis based on the test results.

The draft matrix of 15 test conditions for 30 percent MEA is presented in Table 18. The results will form the baseline performance for comparison with other solvents. The CO_2 capture efficiency is expected to vary between 65 and 95 percent. Modeling results from Promax chemical process simulation software will be used to refine the test conditions. The same methodology will be used to support developers in establishing their matrix of test conditions. If the conditions proposed for MEA in Table 18 were used for an improved solvent the CO_2 capture efficiencies would be higher and the range covered would be reduced. To cover a similar range of capture efficiencies as for MEA, test conditions will have to be redefined.

Table 18. Draft Test Matrix for 30 Percent MEA Testing.

Run	L/G Ratio(1), gal/1000 acf	Gas Flow Rate, lb/hr	Lean Amine Flow Rate, gpm	S/L Ratio,(2) gpm
1	25	5000	22.7	0.7
2	25	5000	22.7	1.0
3	25	5000	22.7	1.3
4	45	5000	40.8	1.3
5	45	5000	40.8	1.0
6	45	5000	40.8	0.7
7	35	5000	31.7	0.7
8	35	5000	31.7	1.0
9	35	5000	31.7	1.3
10 (3)	35	5000	31.7	1.3
11 (3)	35	5000	31.7	1.0
12 (3)	35	5000	31.7	0.7
13	35	2500	15.9	0.7
14	35	2500	15.9	1.0
15	35	2500	15.9	1.3

(1) Ratio of lean amine to flue gas
(2) Ratio of steam to rich amine
(3) Intercoolers in use for these three test conditions only

For the first three tests, the flow rate of lean amine and flue gas to the absorber are held constant and S/L is adjusted by changing the steam flow rate to the regenerator reboiler. For the next two sets of three tests, the lean amine flow rate is increased for the same flue gas flow rate to test the effect of increasing L/G ratio. The fourth set of three tests is similar to the third but with the two absorber intercoolers in service to modify the absorber vertical temperature profile. In the fifth set of tests, L/G is maintained but at a lower flow rate of flue gas and lean amine to determine the effect of absorber gas velocity upon CO_2 capture efficiency.

Second-order variables that might be investigated include absorber gas inlet and outlet temperatures, absorber lean solvent inlet temperature, regenerator rich solvent inlet temperature, and the location to which the reflux is returned to the regenerator.

The process variations occurring following each transition in test conditions will be closely monitored to identify when steady conditions are re-established, indicating the start of the next test condition. In addition to temperatures and pressures throughout the absorber-regenerator, parameters to be monitored include:

- Liquid levels in vessels
- Flow rate of flue gas entering and leaving the absorber
- CO_2 content of flue gas leaving absorber
- Flow rate of CO_2 leaving regenerator
- Flow rate of steam to reboiler
- Flow rate and CO_2 content of rich amine leaving absorber and lean amine entering
- The CO_2 contents can be determined by chemical analysis or inferred from the density of the amine determined by the Coriolis mass flow meter

Once these parameters reach steady state, the solvent contained within the absorber-regenerator will be displaced again, after which the next test period can proceed.

Analytical Procedures for Gases. The gas analyzers used and their location are listed in Table 19.

Table 19. PSTU Gas Analysis Techniques.

Stream	Species	Technique
Absorber Inlet	Oxygen	Zirconia sensor
	CO_2	NDIR
	Moisture	Capacitance
	SO_2	Ultra violet
Absorber Outlet	Oxygen	Paramagnetic
	CO_2	NDIR/FTIR
	Moisture	FTIR
	NH_3	FTIR
	NO_x	FTIR
	NO	FTIR
	NO_2	FTIR
	Amines	FTIR/condensation
Regenerator Outlet	Moisture	Capacitance
	CO_2	By difference

All the techniques used are commercially established. The sensor in the zirconia probe used to measure the oxygen in the absorber inlet flue gas operates at 1,470°F. As the PSTU may use flammable solvents, the high temperature of the zirconia sensor was considered a potential explosion hazard so a paramagnetic sensor was selected for this location.

The FTIR was selected primarily for its ability to simultaneously measure multiple components (amines, water, ammonia, formaldehyde), and the ability to measure a wide range of concentrations (high percent levels to low ppmv levels). An infrared beam is directed into a cell, which determines how much is absorbed by the passing gas stream. A Fourier transform converts the data into a spectrum that the device recognizes provided the spectrum for that species is loaded into the instrument library. The heights of the peaks for the measured spectrum indicate the amount of material present. The device consists of a single cell with eight real-time output signals. Over thirty spectra are included in the library, and the collected data can be analyzed at any time following testing. The cell operates at 360°F, which is considered too low a temperature to pose a hazard.

The gas sample passing to the FTIR comes from a fixed location. Amine transmissions are considered to pose a health hazard, and measurement of this species will be closely scrutinized. To ensure that the FTIR amine determination is representative of the value for the complete duct, an isokinetic extractive system will be used with perpendicular traverse paths. The condensable material present in the extracted gas streams will be collected for the complete traverse and analyzed for its amine content.

Analytical Procedures for Liquids. Table 20 lists the liquid analyzers used and their locations.

Table 20. PSTU Liquid Analysis Techniques.

Stream	Species	Technique
Absorber Inlet and Regenerator Outlet	CO_2	Auto-titration with KOH (established for lean solvents)
	MEA	Auto-titration with HCL (not applicable for blended amines)
	Amine blends	Batch analysis using GC (proposed method not yet validated)
	Moisture	Titration with KF
Absorber Outlet, Regenerator Inlet, and Intercooler Loops	CO_2	Auto titration with KOH (experimental method for rich solvents)
	MEA	Auto-titration with HCL (not applicable for blended amines)
	Amine blends	Batch analysis using GC (proposed method not yet validated)
	Moisture	Titration with KF

An auto-titration system is used to determine the amine content of the aqueous solution and also its CO_2 content. Titrating with HCl determines the alkalinity of the solution and hence the total amount of amine present. If a single amine, such as MEA, is used then the measurement is satisfactory. However, if a blended amine is used, the measurement cannot determine the proportions of the different components present, and so the mixture composition cannot be accurately determined with this method.

To determine the composition of blended amines, a batch sample will be taken and analyzed in the laboratory using a GC. Initial work with MEA, diethanolamine, methyldiethanolamine, morphaline, and piperazine has yielded accuracies within 5 percent.

Titrating with KOH to determine CO_2 content will work reliably for the cooled lean amine entering the absorber. The issue with the rich amine leaving the absorber is that extracting the sample will lower the pressure, flashing off some of the CO_2 resulting in a faulty measurement.

To prevent flashing, the sample will be cooled to room temperature prior to pressure reduction. This approach has not yet been tested, and for some solvents, it may not be acceptable. For example, piperazine when cooled may solidify, blocking the sample line. If the CO_2 content of the rich amine cannot be measured, it can be calculated from the incoming lean amine CO_2 content and the amount of CO_2 absorbed.

Quality Assurance (QA) Procedures. To ensure the accuracy of mass and heat balances and process performance parameters, quality control (QC) checks will be used to verify the accuracy of measured flue gas and CO_2 flow rates, flue gas CO_2 concentrations, solvent flow rates, and solvent CO_2 loadings. Table 21 lists these procedures.

Table 21. PSTU Quality Assurance Procedures.

Measurement	Method	Location	QC Check
Flue Gas Flow Rate	Annubar	Absorber gas inlet and outlet	Periodic traverses with S-type pitot tube
CO_2 Flow Rate	Annubar	Regenerator outlet	Periodic checks with fixed position pitot
Flue Gas CO_2 Concentration	On-line NDIR	Absorber gas inlet and outlet	Zero and span daily re-calibrate as necessary
Solvent Flow Rate	Coriolis meter	Lean solvent inlet and rich solvent outlet	Volumetric or gravimetric checks; Off-site calibration of meters
Solvent CO_2 Loading	Auto titration	Lean solvent inlet and rich solvent outlet	TCA*, carbon mole balance, and lab titration

*Total CO_2 analysis

The flue gas enters and leaves the absorber in 10-inch diameter ducts and allow for pitot traverses in two directions perpendicular to each other. The CO_2 leaves the regenerator in a 3-inch pipe so an accurate determination can be achieved with a fixed location.

Auto-titration analyses of the solvent CO_2 loading will be checked using periodic laboratory titrations, carbon mole balance calculations, and the Total CO_2 Analysis (TCA) procedure. This technique, illustrated by Figure 41, was developed at the University of Texas and refined at the NCCC, and has been shown to give accurate measurements of the CO_2 loading in various known standard solutions. The CO_2 present in the sample is liberated by adding sulfuric acid solution. A metered flow of nitrogen sweeps the CO_2 into a continuous analyzer, and the output signal is integrated to determine the total amount of CO_2 contained in the sample.

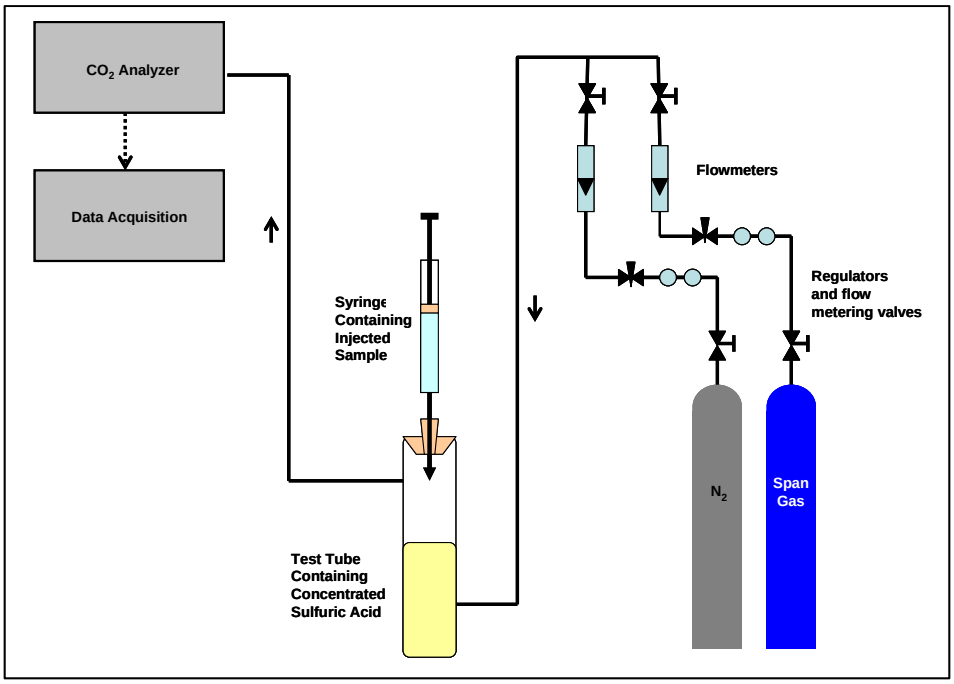

Figure 41. Total CO_2 Analysis Apparatus.

In addition, the QA plan calls for separate procedures to assess the accuracy and precision of various analytical methods that will be used at the PSTU. Table 22 provides a summary of the proposed techniques for assessing analytical accuracy and precision.

Table 22. Proposed Techniques for Assessing Analytical Accuracy and Precision.

Analysis	Method	Accuracy	Precision
Total CO_2 Loading	Auto titration, lab titration, and TCA	Standards and spikes in amine	Periodic triplicate samples
Amine Reaction/ Degradation Products	FTIR, GC/MS, HPLC, IC, ICP/MS, NMR, QTOF/MS	Standards and spikes in amine	Periodic triplicate samples
Anions	IC	Anion standards and spikes in amine	Periodic triplicate samples
Metal Cations	AAS, ICP/MS	Certified reference materials (single- or multi-element)	Periodic triplicate samples

AAS atomic absorption spectrometry
FTIR Fourier transform infrared spectroscopy
GC/MS gas chromatography-mass spectrometry
HPLC high-performance liquid chromatography
IC ion chromatography
ICP/MS inductively coupled plasma mass spectrometry
QTOF/MS quadrupole time-of-flight mass spectrometer

To assess the accuracy of auto-titration, laboratory titration, and TCA, known carbonate standards (e.g., K_2CO_3) will be used in aqueous solution and added as a spike to the amine or other solvent. The CO_2 loading measured by the analysis should be within 5 percent of the known CO_2 content on a relative basis. If not, a new calibration curve will be generated and

applied. A similar approach will be used for the various techniques used to analyze amine reaction and degradation products, except that the standards and spiking compounds will be reagent-grade versions of the actual reaction/degradation product.

Other procedures being developed for the QA plan include:

- Requirements for the training of analytical personnel
- Corrective actions to be taken when QC checks fall outside of acceptable ranges
- Procedures for labeling samples and maintaining proper sample chain of custody
- Procedures for reporting results

Consistent application of the above procedures to all of the analytical work, flow measurements, and gas analyses will ensure that the results produced are of the highest possible quality.

Analysis of Degradation Products. Knowledge of the compounds present in the degradation products is needed to understand the degradation mechanism, to support work to minimize degradation, and to understand the environmental implications of amine waste product disposal. Some of the MEA degradation products reported in the literature include various acids (acetic, formic, oxalic, propionic, and butyric); amides (formamide and lactamide); aldehydes (formaldehyde, acetaldehyde, and imidazole carboxaldehyde); ketones (oxazolidone and imidazolidone); nitrosamines; certain anions (nitrate and nitrite); and ammonia.

The solvent may also be analyzed for certain cations to check for contamination from corrosion products, residual fly ash, and solids carried over from the SO_2 scrubber. These analyses would be carried out using ICP-MS, and accuracy would be checked using certified single- or multi-element reference materials provided by the National Institute of Standards and Technology (NIST). To check analytical precision, the various analyses will be periodically run in duplicate or triplicate.

4.2.2 PSTU COMMISSIONING

Effective commissioning of new equipment bridges the gap between construction and safe operations. As part of this effort, the NCCC created a startup team to schedule, train, and develop procedures in preparation for commissioning efforts later in the year. The startup team worked closely with the construction and design groups to effectively prepare equipment for normal operations. Also, the startup team developed and delivered training on operation of the PSTU and BOP equipment. Documentation was written for commissioning, startup and operation of equipment, and safety and environmental guidelines. Process controls were configured and tested, and operating graphics were developed for operation of the units. Preparation began for the installation and operation of gas and liquid analyzers for the PSTU. Finally, systems that were turned over from construction were commissioned, including checkout of the PSTU.

Planning and Scheduling. An important component of the commissioning process is integrating the commissioning schedule with the construction schedule. Construction schedule changes are inevitable, so the startup team worked closely with the design and construction group to

prioritize work, maintain schedule and control costs. The startup team revised and optimized commissioning packages as necessary to meet intermediate milestones, such as commissioning baseline BOP utilities and circulating water through the PSTU.

Documentation. The PC4 startup team developed the necessary documentation for commissioning packages, startup and operation of equipment, and safety and environmental guidelines. Commissioning packages included pipe flushing and hydro test instructions, associated drawings marked to assist in steps, and preparatory checklist. These packages were developed for 19 subsystems within the BOP and PSTU. Operating procedures for startup, shutdown, and standard operations were also developed for BOP and PSTU equipment. Because the PC4 system is located on an Alabama Power plant site, it requires safety and environmental guidelines separate from the rest of the NCCC/PSDF facility. Safety and environmental guidelines were developed that include an emergency action plan, waste disposal guidelines, personal protective equipment recommendations, and spill response instructions.

Training. In preparation for operating and maintaining PC4, training was delivered to prepare operations and maintenance staff to work safely in the unit. Hazard communications training was delivered by safety, environmental, and technical staff to personnel scheduled to work at PC4. Additionally, operations and maintenance staff received an introductory course on the PC4 operations.

Process Controls. The PSTU is a highly automated process requiring extensive controls, instrumentation, and control graphics. Balance of plant equipment supplies the necessary utilities for operation of the PSTU and other operating units at PC4. Initial setup and checkout of this equipment was completed, with necessary controls and instrumentation functional to operate the potable water, filtered water, cooling water, instrument air. Also, the majority of control loops and instrumentation in the PSTU were checked. Approximately 400 electrical wiring loops, 100 automated valves, and 60 control graphics were designed, and checkouts were underway during the last quarter of BP2.

Commissioning. Equipment commissioning began in the fall, with the following systems commissioned successfully: power supply, fire water, potable water, filtered water, cooling water, instrument air, and the PSTU. Operations performed a hydrodynamic test with water and air on the PSTU as an initial check of the equipment.

The water run was a critical component of commissioning efforts for PC4, allowing check out of major components of the system and insight into unit operations. All major liquid circuits were operated continuously for 10 days. Leaks were found and repaired (mostly loose flanges). Liquid circuit control loops were tuned during this time as well. Mechanical and instrument issues were identified and will be resolved before the baseline solvent test. Examples include faulty flow switches, improper gasket materials, incorrect pressure differential transmitter installations, and a drainage issue with the rich/lean solvent heat exchanger. Column packing in the absorber and regenerator were cleaned (to remove cutting oil) with a low concentration amine (5 wt%) for 24 hours. The cleaning solution was tested for pH (pH ranged from 10-11, which is acceptable for discharge), drained, and the system was rinsed again with water. After the water run, all systems were drained and winterized. Additionally, the flue gas blower was

operated, and flue gas piping was charged with air to check for leaks. Minor leaks were identified for repair, and control valves were checked out.

The following systems at PC4 need to be commissioned in 2011 prior to testing of the PSTU: the steam system, flue gas supply, chemical preparation, nitrogen supply, and gas/liquid analysis.

4.3 PLANNED TESTING IN 2011

The planned testing at PC4 during 2011 is listed in Table 23. The periods identified are provisional. At this time, the developers will not be identified, pending signing final agreements.

Table 23. PC4 Tests Planned for 2011.

Test	Provisional Intervals
Commissioning and Operation of PSTU to Establish Baseline Test Data with MEA	March to May
Commissioning and Operation of PSTU with Developer A's Solvent	June to July
Operation of Sorbent Test Skid	August to September
Operation of Developer's Solvent Test Module	April to September
Operation of Developer's Membrane Test Module	October to November
Commissioning and Operation of PSTU with Developer B's solvent	September to November

5.0 GASIFICATION PROCESS

The PSDF gasification process, represented in Figure 42, features key components of an IGCC plant. These include high pressure solids feed systems; a Transport Gasifier; syngas coolers; a hot gas filter vessel, the particulate control device (PCD); and continuous ash depressurization systems developed at the PSDF for ash cooling and removal.

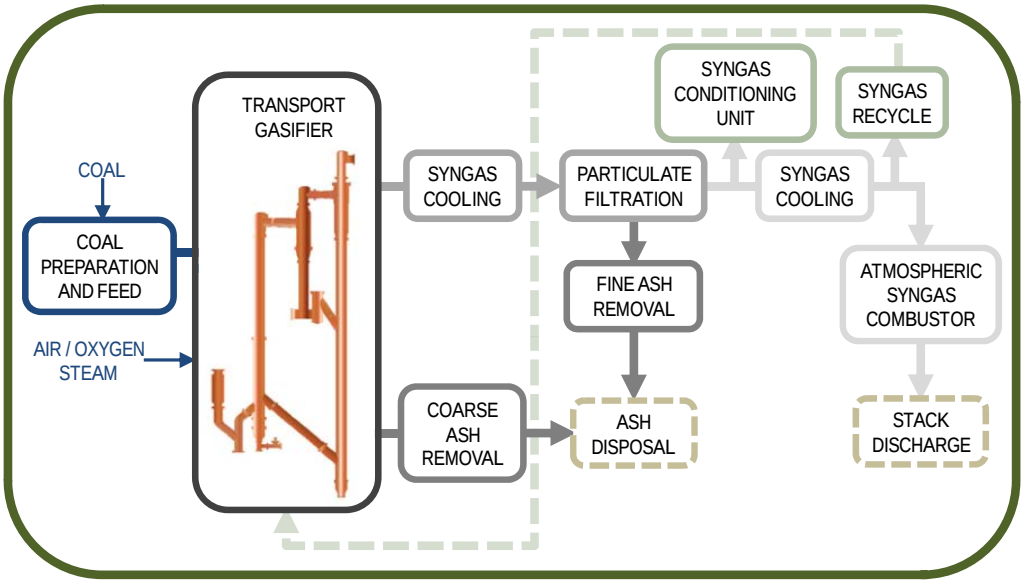

Figure 42. Flow Diagram of PSDF Gasification Process.

Operation of the gasification process occurred over three test runs during BP2—test runs R03, R04, and R05—for a total of 2,088 hours. While R03 began in Budget Period One, it was completed in BP2, and so the results are included in the BP2 report. The original test plans for BP2 included an additional 500-hour run, R06. However, the plans were changed to combine the two 500-hour runs into the one extended 1,000-hour run, R05.

At the conclusion of R05, the gasification process had operated for over 14,600 hours on coal. The test runs provided the opportunity to test processes specific to gasification, as well as to provide syngas for SCU testing.

5.1 DEVELOPMENTAL COAL FEEDER

Over test runs R03 through R05, the developmental Pressure Decoupled Advanced Coal (PDAC) feeder operated under these conditions:

- Total operating time of over 1,850 hours
- Operation as the sole coal feeder for 67 hours
- Feed rates from 500 to 5,700 lb/hr

Improvements to the feeder control logic were ongoing throughout the reporting period. These improvements are discussed below.

Optimizing the Lock Vessel Filling Cycle Using Level Probe Indications. Vibration-type level probes (discussed in Section 5.3.3), which were installed on the feeder dispense vessel and lock vessel prior to R02, reliably detected coal level in both vessels and proved a more reliable indication than the capacitance probes used previously. As a result of the increased reliability, the lock vessel filling cycle was optimized to use the level probe indication to end the fill cycle instead of waiting for the timer to time out. The benefit of this change is especially significant when operating the feeder at higher feed rates.

Tuning to Maintain Steadier Dispense Vessel Pressure. This tuning was needed to minimize the impact of lock vessel fill cycles on feed rate variability. The process included the addition of a feedback controller to adjust coal feed rate when gasifier pressure changes are made. The controller monitors set point changes in gasifier pressure and triggers the addition or venting of process gas to the feeder in order to maintain a constant coal feed rate.

Tuning of the Instantaneous Coal Feed Rate Feedback Control. The instantaneous coal feed rate feedback control was tuned to further improve response to sudden changes in feed rate. Optimization of the control resulted in decreased feed rate variability as indicated by the conveying line differential pressure indication. Future testing will involve the incorporation of the new DensFlow coal flow meter (discussed in Section 5.3.2) into the control scheme.

Optimizing Storage Silo Operating Level. Control changes were also made to increase the operating level of the feeder atmospheric storage silo. Controlling the silo at a higher level promoted a mass flow regime from the bin, decreasing material segregation that can lead to coal feed rate fluctuations.

5.2 BIOMASS EVALUATION

The gasification system operated for the first time co-feeding biomass with coal in test run R03, and further testing was completed in test run R04. Co-gasification operation took place for 200 hours during R03 using PRB coal with the biomass, and in R04, biomass was co-fed with lignite coal for 100 hours. The biomass was purchased in the form of wood pellets (see Figure 43), supplied by Green Circle Bio Energy, which were milled and fed to the pressurized gasifier in a dedicated feeder at rates from 500 to 2,500 lb/hr, about 20 weight percent of the total feed rate. Operation of the biomass/coal blends yielded steady state carbon conversions averaging over 99 percent.

Figure 43. Wood Pellet Biomass Used as Gasification Feedstock in R03 and R04.

The NCCC conducted the biomass testing to support the DOE goal of development of gasification technologies for the conversion of biomass into clean, sustainable energy and other products. The biomass testing at the facility is also in harmony with Southern Company's extensive testing over the last several years of energy production from biomass, which the company considers to be a promising resource for producing renewable energy cleanly and efficiently.

Successful operation with the biomass/coal blend required the NCCC staff to address several challenges associated with feeding and gasifying biomass. First, because biomass is fibrous, it can be difficult to pressurize and reliably convey. Second, compared to coal, biomass ash can be more prone to agglomerate at gasifier conditions and has the potential to be corrosive. Last, biomass gasification can lead to excess tar formation, which can foul downstream equipment. After assessing the available biomass options, wood pellets were selected for testing because they are currently produced on a commercial scale, the particle size and low moisture content of milled pellets make the material suitable for existing coal mills and feeders in the gasification process, and the low ash and chlorine content reduces the risk of ash agglomeration and corrosion issues.

Preliminary testing completed during 2009 consisted of milling and feeding the biomass at rates from 400 to 3,000 lb/hr in a pressurized off-line system (independent of the gasification process), and showed that reliable feeding could be achieved. Laboratory studies of biomass co-gasification included agglomeration testing, during which blends of biomass and coal ash at varying weight ratios were baked in a muffle furnace at typical gasifier operating temperatures. The baked samples were examined visually, by optical microscopy, and by scanning electron microscopy with energy-dispersive X-ray analysis for signs of agglomeration tendencies. The laboratory testing indicated that the biomass was not prone to agglomeration and was suitable for further testing in the gasification process. By adjusting the process parameters according to the preliminary test data, the gasification process operated with reliable feeding and with no evidence of ash agglomeration, corrosion, or excessive tar formation.

5.2.1 BIOMASS FUEL HANDLING AND FEEDING

The biomass was milled using the existing roller mill systems. Table 24 lists the R03 and R04 biomass moisture and particle size data before and after milling. A few modifications were made to the mill operational settings for system air flow and mill speed to effect the final particle size distribution. Additionally, system pressure was decreased to raise air flow rates in order to improve material feed from the mill outlet cyclone collector to the pulverized silo. This change was necessary due to the difference in physical properties of biomass relative to coal.

Table 24. Biomass Properties before and after Milling.

Biomass Property	Average Value	
	R03	R04
As-Received Moisture Content, wt %	7	7
As-Fed Moisture Content, wt %	4	4
Moisture Content Reduction, %	43	43
As-Fed Mass Median Diameter, micron	930	830
As-Fed Oversize (>1,180 micron) Content, wt %	38	29
As-Fed Fine (<45 micron) Content, wt %	11	1

While mill system operation was satisfactory, problems occurred during R03 with the dense phase pneumatic conveyor that transfers the processed biomass from the mill system pulverized storage silo to the coal feeder storage silo. The root cause of the transfer problems was a combination of flow restrictions in the discharge piping and insufficient conveying gas supply. First, the discharge piping layout was not conducive to the transfer of a lower density fibrous material such as biomass, as it contained several long radius elbows that reduced the velocity of the material enough to cause it to collect along the bottom of the piping, eventually forming a plug in the line. The fibrous structure of the biomass allowed the individual particles to compress and interlock with one another, forcing them outward against the pipe wall and preventing the material from transferring. This occurrence had not been observed in previous operations when conveying coal from the pulverized silo to the feeder due to its non-compressible nature. The second and equally important cause for the transfer problem was that the system had an insufficient supply of conveying gas (nitrogen) to maintain conveying velocity of the biomass particles high enough to prevent line plugging.

Both of these problems were mitigated during the run by decreasing the amount of biomass charged to the conveyor and by re-arranging and adding conveying gas to the system. During the outage between run R03 and R04, modifications were made to the dense phase conveying system that transfers the biomass from the pulverized coal storage silo to the coal feeder. The piping layout was modified to remove excess elbows and other areas of unnecessary pressure drop. Additionally, the conveying gas supply to the dense phase feeder was increased and booster gas was added to elbows in the transfer line. For the transfer line booster gas additions, new Kates flow controllers were installed that maintain a constant volumetric flow of gas by using an internal regulating valve to counterbalance downstream fluctuations in pressure. These changes resulted in improved system operation when compared to R03 operation, maintaining solids velocity requirements high enough for consistent transfer of the low density biomass material. Figure 44 shows some of the changes made.

Figure 44. Modifications to the Dense Phase Transfer Line for Biomass Conveying.

While it is recognized that the dense phase conveying is not as well-suited for this application as other pneumatic conveying methods (i.e., dilute phase conveying with higher gas to solids ratios), the modifications incorporated provided the most economical path to successful conveying of the biomass at this facility.

Off-Line Biomass Feeder Testing. A milestone to perform off-line testing with different biomass/coal was incorporated in the project plan to support testing of co-gasification of biomass with coal during R03 and R04. While the wood pellets that were tested during R03 (from forest waste) were different in physical properties from the pellets tested in the off-line system in early 2009 (made from recycled furniture), the biomass was successfully fed during R03 for more than 200 hours without any operational problems in the gasifier. The prospect of testing a torrified biomass material was investigated but there were concerns about the economic viability of a commercial plant using this expensive material, plus the material could not be acquired during the available time frame. Based on the unavailability of the alternate biomass and the success during R03, plans were made to move forward with another co-feed test in run R04 with a different coal/biomass feed of Mississippi lignite and the wood pellets without another off-line test.

5.2.2 GASIFIER OPERATION

Gasifier operation during coal only feeding and during co-feeding of coal and biomass yielded high carbon conversions, as shown in Table 25.

Table 25. Steady State Carbon Conversions for R03 and R04.

	Maximum		Minimum		Average	
	R03	R04	R03	R04	R03	R04
Coal Only Carbon Conversion, %	98.7	99.9	97.1	97.6	98.3	99.1
Biomass Co-Feed Carbon Conversion, %	99.6	99.9	98.9	99.3	99.2	99.6

Inspections of gasifier ash samples taken during coal-only feed and during co-feeding periods did not indicate agglomeration (see Figure 45). Additionally, the primary gas cooler performance remained stable, and condensate sampling did not indicate any evidence of tar formation.

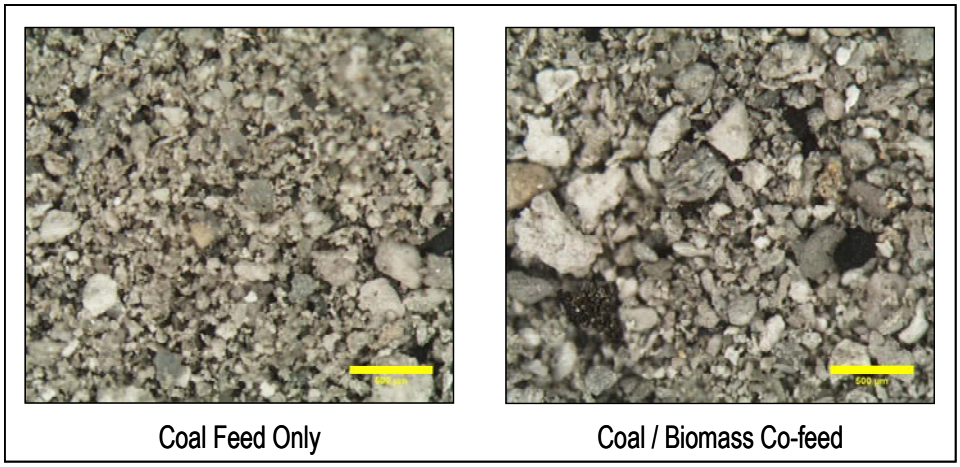

Figure 45. Gasifier Ash Samples during Coal-Only Feed and during Biomass Co-Feed in R04.

During the final hours of test run R04, a period of biomass feed only was tested. Primary gas cooler performance began to deteriorate soon after establishing biomass only feed to the gasifier, as the cooler outlet temperature began to rise (evidence of tube fouling). Eventually, this decrease in performance resulted in the end of gasifier operations for R04. Post-run inspections revealed fouling in the primary gas cooler tubes, as shown in Figure 46. Samples from the tubes were collected for analysis, and results indicated the presence of tars. A secondary test of the tube foulant did not reveal any alkali metal content which can also provide a mechanism for fouling. For biomass co-feed operation in the future, a more gradual transition to biomass only feed is planned to better understand when the increased tar generation problem begins.

Figure 46. Post-Run Inspection of Primary Gas Cooler Tubes.

5.2.3 EFFECT OF BIOMASS CO-GASIFICATION ON ASH CHARACTERISTICS

Table 26 lists the characteristics of the ash entering the particulate control device (PCD) during gasifier operation with and without biomass co-feeding. Because of the low ash content of the biomass, the addition of biomass reduced the inlet ash concentration with both the PRB coal and the Mississippi lignite. The addition also increased the bulk density and true density of the ash, while reducing the bulk porosity and surface area. The loss on ignition was also reduced, suggesting that the biomass addition improved carbon conversion. There was no significant effect on mean particle size of the ash as this is controlled primarily by the performance of the gasifier solids separation devices.

Table 26. Effect of Biomass Co-Gasification on Ash Characteristics.

Gasifier Fuel	Bulk Density, g/cm^3	True Density, g/cm^3	Bulk Porosity, %	Loss on Ignition, %
PRB Coal (R03)	0.25	2.64	90.5	19.2
PRB Coal (R05)	0.31	2.64	88.2	16.5
PRB Coal and Biomass (R03)	0.35	2.74	87.2	9.8
MS Lignite (R04)	0.45	2.62	82.8	10.3
MS Lignite and Biomass (R04)	0.52	2.77	81.1	2.1

Effect of Biomass Addition on Particle-Size Distribution. Figure 47 shows the effect of biomass addition on the particle-size distribution of ash entering the PCD as measured by Microtrac laser diffraction analysis of the PCD inlet ash samples.

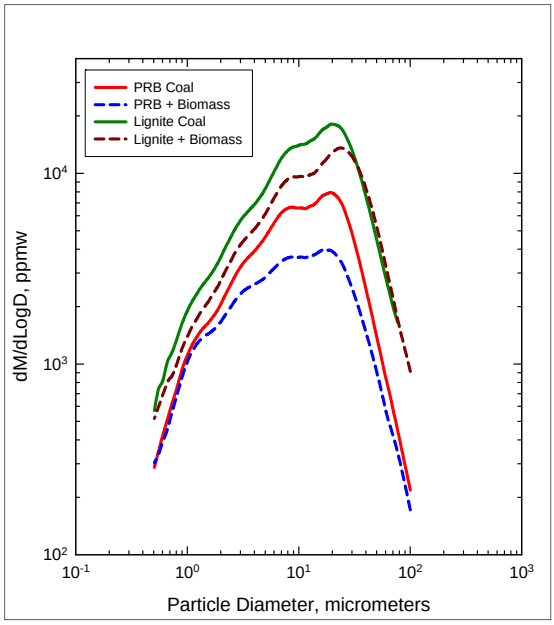

Figure 47. Particle-Size Distributions of Ash Measured at PCD Inlet.

The results are presented as a series of differential mass distributions that represent a differentiation of the cumulative mass loading curve. This type of presentation is widely used with fine particle measurements, because the dM/dlogD value reflects the mass concentration of particles in a given size band, and the area under the curve between any two points indicates the mass concentration of particles within that particle size range. As indicated in Figure 47, the addition of biomass reduced the mass concentration of ash over almost the entire particle size range. With PRB coal, the mass reduction occurred over the range of about 1 to 50 microns. With Mississippi lignite, the reduction was evident over the range of about 0.5 to 30 microns. Little difference is seen in the distributions at the upper end, because those particles are largely removed by solids separation section of the gasifier.

Effect of Biomass Addition on Transient Drag. Past studies showed that dustcake drag generally decreases with decreasing ash carbon content (or decreasing loss on ignition). Since the loss on ignition was reduced by the addition of biomass, a commensurate reduction in the dustcake drag was expected. The transient drag of the dustcake is calculated from the transient pressure drop, the ash mass loading, and filter face velocity (based on syngas flow) using procedures presented in earlier reports. (Transient pressure drop is the pressure drop increase between pulse-cleaning cycles.). In keeping with previous results, the drag was proportional to the ash carbon content (loss on ignition) as indicated in Figure 48. The lignite ash has lower drag than that of the PRB due to differences in ash morphology and the slightly larger particle size of the lignite ash resulting in less flow resistance. For both fuels, the lowest drag occurred with coal and biomass co-feeding. Based on these results, the addition of biomass would not have an adverse effect on PCD pressure drop.

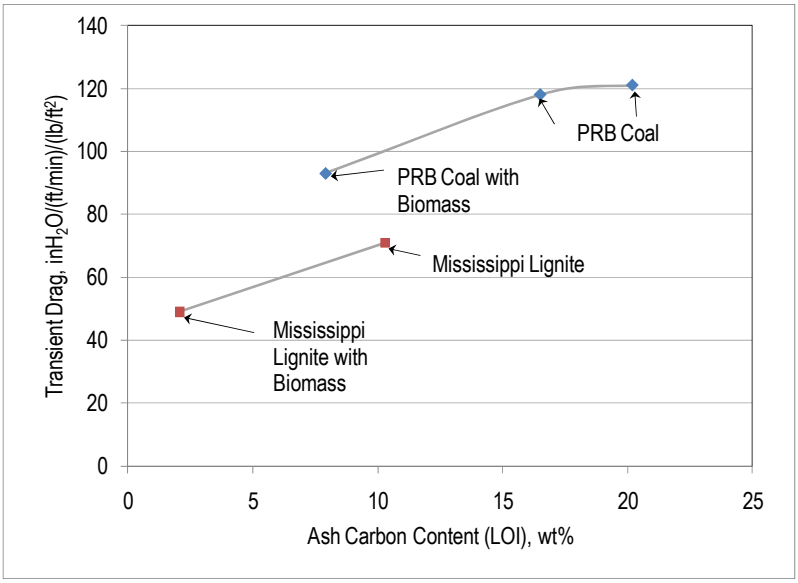

Figure 48. Transient PCD Drag as a Function of Carbon Content.

Laboratory Drag Measurements. Figure 49 shows dustcake drag as a function of particle size using the re-suspended ash permeability tester in the on-site laboratory. In these measurements, the ash samples obtained with and without biomass addition are re-suspended in a fluidized bed and

passed through various combinations of small cyclones to produce ashes with a range of particle sizes. The ash from the cyclones is collected on a sintered metal plate. Monitoring the flow and pressure drop during the build-up of the dustcake on the sintered plate and weighing the collected cake allows the dustcake drag to be determined as a function of particle size.

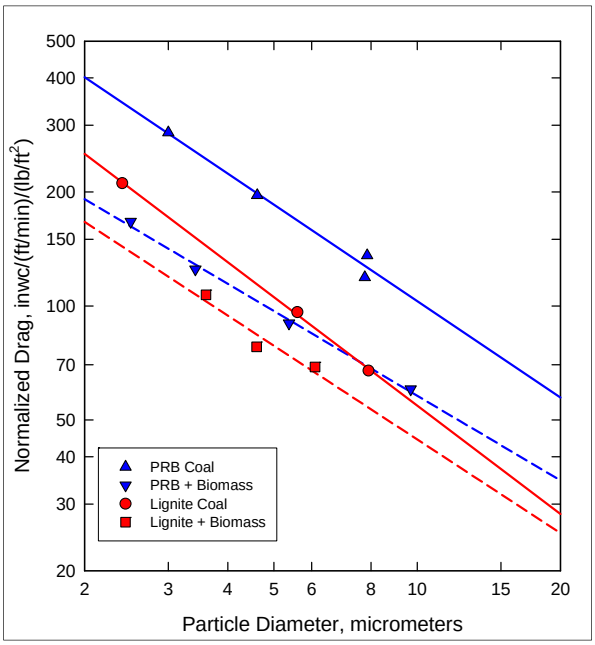

Figure 49. Effect of Biomass Addition on Laboratory Drag Measurements.

As shown in Figure 49, the dust cake drag with both the PRB coal and Mississippi lignite is lower for ashes with biomass addition over the particle size range studied (approximately 2 to 10 microns). This difference is considered to arise primarily from the effect of carbon content shown in Figure 48. From the two figures, it can be concluded that the transient drag of the dust cake is inversely proportional to its mean particle size and proportional to its carbon content, although there is also likely a contribution from other morphological differences.

5.3 SENSOR DEVELOPMENT

Because of the research nature of the NCCC/PSDF and the unique process conditions, significant effort has gone into the development of instrumentation. During BP2, sensor development included a sapphire thermowell for gasifier service, a coal flow measurement device, and coal feeder level probes.

5.3.1 SAPPHIRE THERMOWELL

A sapphire thermowell was installed in the gasifier riser prior to run R04 to test the durability of this material in a high-velocity, erosive environment. The performance of the sapphire thermowell was compared with an existing HR-160 thermowell installed in the same plane of the gasifier. Both thermowells contained Type-N thermocouples which have an accuracy of +/- 0.75 percent. The percent difference between the average steady state temperature

indications of the thermocouples averaged about one percent during R04 and averaged about 3.5 percent during R05. Figure 50 illustrates the agreement of the two indications.

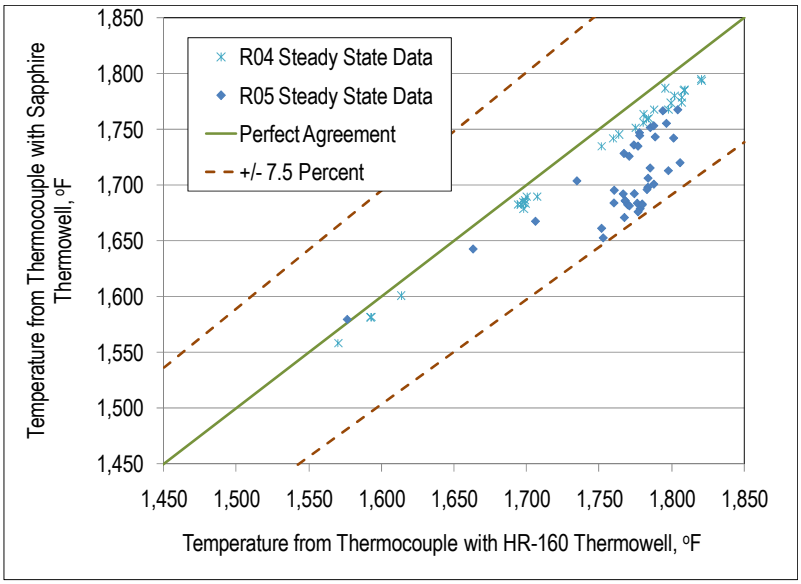

Figure 50. Comparison of Temperature Readings for Sapphire and HR-160 Thermowells.

Post-run inspections of the thermowell revealed no signs of erosion or ash deposition. While the percent difference between the two temperature indications at the beginning of R05 was close to the expected accuracy for the thermocouple type, the sapphire thermowell indication began to drift low about 330 hours into the run. Based on this observation, thermowell condition and/or a temperature transmitter problem were thought to be the cause. The temperature transmitter will be inspected during the outage to determine if it contributed to the slow decrease in the temperature reading. Additional insight into the observed performance will be pursued with representatives of Emerson Process Management, who supplied the thermowell, pending the outcome of the transmitter investigation.

5.3.2 DENSFLOW COAL FLOW METER

A new coal flow measuring device, the DensFlow meter from SWR Engineering, was installed in the developmental coal feeder discharge line to the gasifier prior to R04. This device is a non-intrusive technique of measuring solids flow using a patented alternating electromagnetic field. The solids flowing through the device absorb this field energy, and a measurement of density of the material is inferred. Simultaneously, conveying velocity is also calculated by the same sensors. The combination of the two measurements with the cross sectional area of the device yields a mass flow rate of material through the feeder discharge line.

Operation of the flow meter during R04 with Mississippi lignite showed good agreement when compared to the existing weigh cell loss of weight calculation. The measurement was also sensitive to instantaneous changes in coal feed rate when compared to existing conveying line differential pressure readings. During R05, the flow meter again displayed good agreement with

the weigh cell calculation at higher flow rates. However, during low feed rates with PRB coal during R05, the agreement was poor. Figure 51 plots the feed rate data for the two runs.

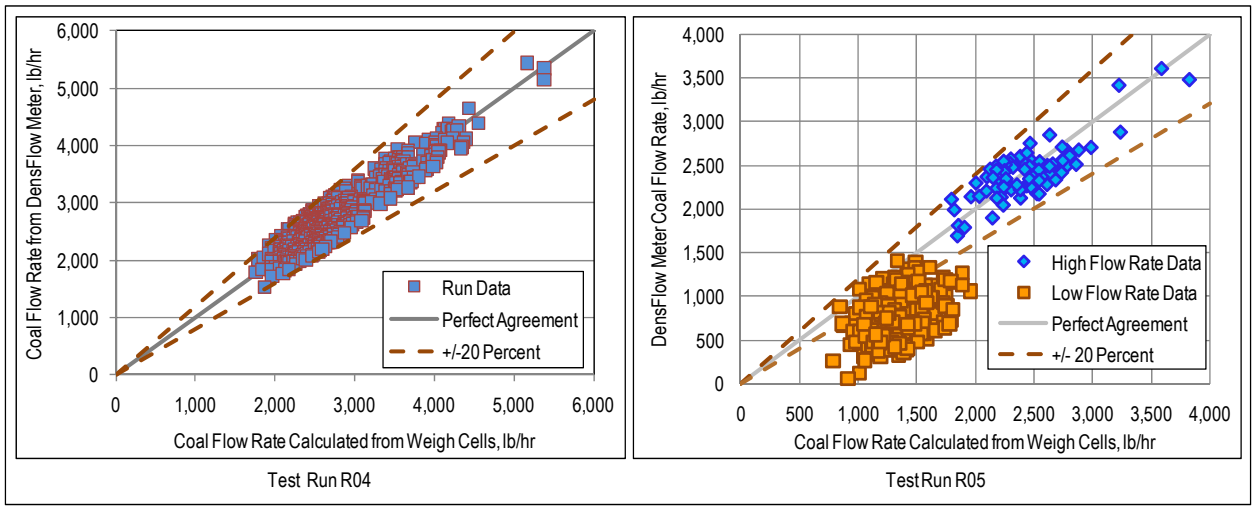

Figure 51. Comparison of Flow Rates from DensFlow Meter and from Weigh Cell Indications.

Discussions with SWR Engineering representatives indicated that the inaccuracy could be due to the change in coal properties, and that recalibrating the probe using PRB coal as the reference material should result in more reliable readings. The meter will be recalibrated for future service with PRB coal.

5.3.3 COAL FEEDER LEVEL PROBES

Dynatrol Level Probes. Long term evaluation of the Dynatrol vibration level probes continued during R04. The probes were installed to replace older, less reliable capacitance probes in several locations including both the lock vessel and dispense vessel of the feeder. The probes continued to demonstrate consistent operation. The vibration probes have a wide range of material measurement capability, from low density flakes or powders to heavy granules and pellets, and there is no required field adjustment of the probes after installation. After R05, the probes had operated for over 2,500 hours providing consistent indication of solids levels inside the vessels for both lignite and subbituminous coals.

Drexelbrook Level Probe. Additional level probe technology was tested in the PDAC feeder dispense vessel during R04. Observations of previous feeder operation revealed a decrease in coal feed rate slightly before a subsequent lock vessel fill cycle occurs. Data analysis of these instances indicated that a deep funnel was forming inside the dispense vessel resulting in the drop in coal feed rate. In order to prevent this occurrence, the dispense vessel needed to be controlled at a higher level. Therefore, a vertical level probe was installed in the top of the dispense vessel to permit the lock vessel fill cycle to occur sooner, maintaining higher level control.

A Drexelbrook point sensitive level probe was selected for this service. The operating basis of the probe is similar to a capacitance probe but combines a radio frequency signal with circuitry

shielding technology to ignore the effects of material buildup on the probe. Initial field calibration of the probe was required using a simple potentiometer adjustment.

Controlling at a higher level helped avoid the development of funnel flow inside the vessel, resulting in a more consistent coal feed rate. However, there were occurrences during which the level probe did not change state causing the vessel to become overfilled. It was determined that the probe had been improperly calibrated prior to R04, causing a decrease in the point sensitivity. After re-calibrating the probe, it was used for dispense vessel level control during the entire R05 run without any instances of vessel overfill.

5.4 GASIFIER PERFORMANCE EVALUATION

Parametric testing was performed during gasifier startup of run R04 (before coal feed) to determine if standpipe fluidization could be used exclusively to control gasifier solids circulation rate to low levels. Test data indicated that gasifier solids circulation rate could be controlled to low levels by varying only the fluidization to the bottom of the standpipe. Figure 52 illustrates the relationship demonstrated during this testing.

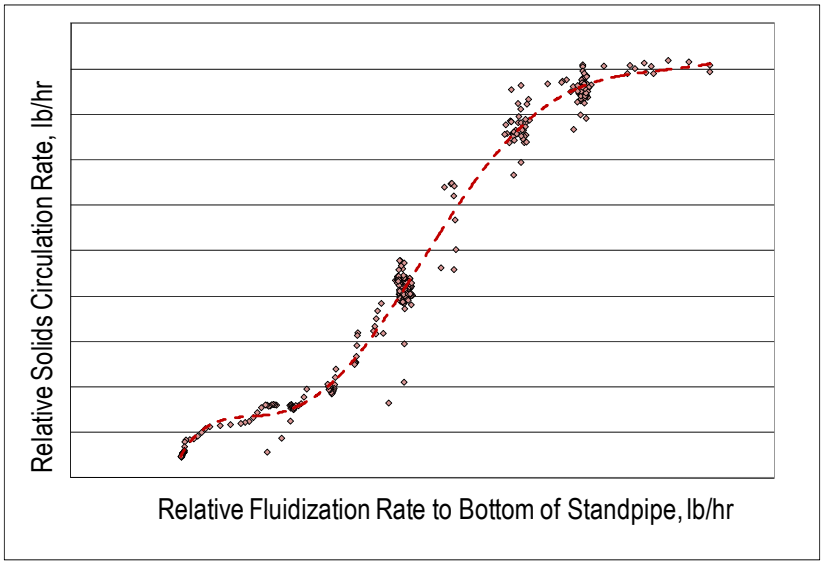

Figure 52. Gasifier Solids Circulation Rate versus Fluidization Rate to Bottom of Standpipe.

A new gasifier temperature control scheme utilizing upper and lower mixing zone air flow adjustments was evaluated during R05. The purpose of this new control scheme was to demonstrate control of gasifier mixing zone temperatures using standard proportional–integral–derivative controllers to adjust air flow to the different zones while maintaining a constant total air flow to the gasifier. The control scheme was further modified during the run to control gasifier exit temperature by adjusting the gasifier total air flow set point. Control loop tuning was performed to modify the responsiveness of the controllers to changes in gasifier temperature set point. Since gasifier upper and lower mixing zone temperatures respond rapidly to changes in air feed rate, the temperature controllers were tuned to respond slowly to minimize temperature overshoot. Figure 53 plots the response to a change in temperature set point.

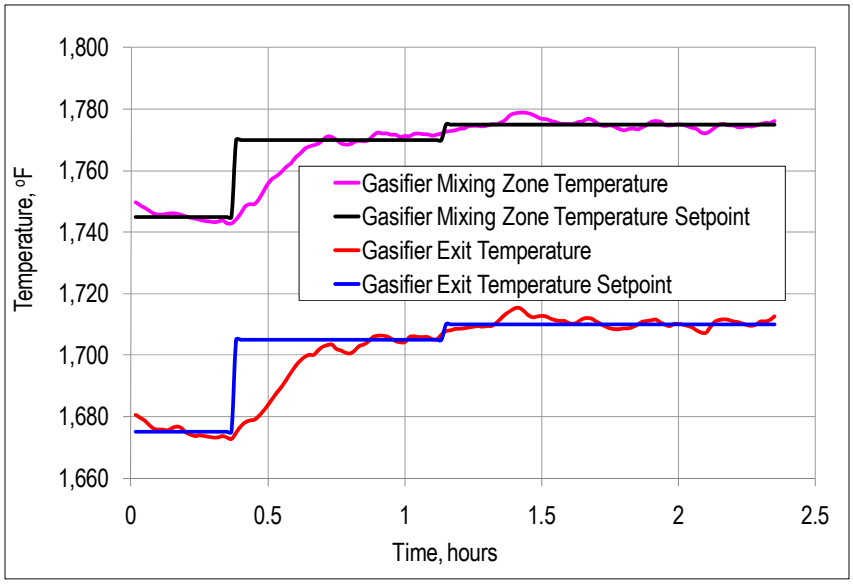

Figure 53. Gasifier Temperature Response to Set Point Change.

Additionally, the controllers were tested to ascertain the ability to maintain a constant gasifier temperature. Figure 54 illustrates the steady state temperature performance. The controllers will be optimized further in future gasification runs.

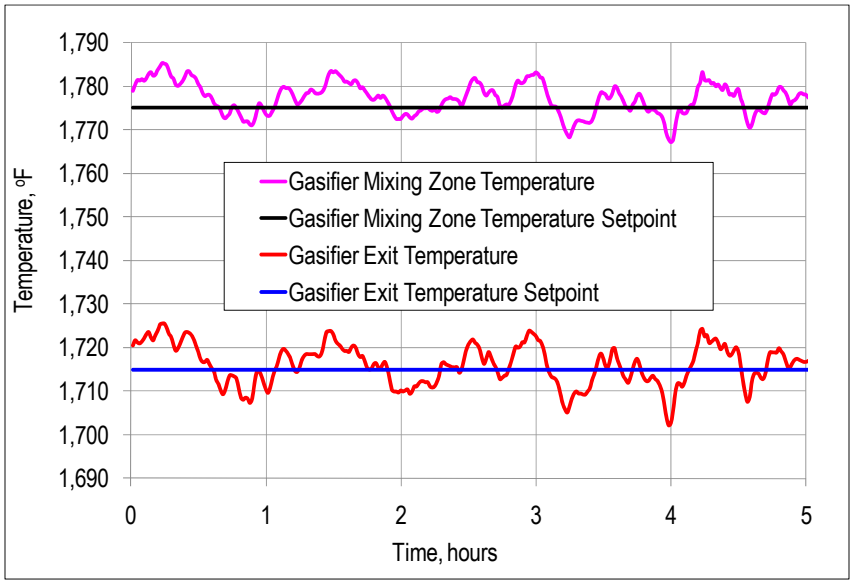

Figure 54. Gasifier Temperature Control Steady State Performance.

5.5 HOT GAS FILTER ELEMENT EVALUATION

During the gasification test runs, the PCD operated with very high collection efficiency (>99.999%) and without any filter element failures. Since the PCD was not opened for inspections during 2010, there was no off-line inspections of the filter elements. A new type of

filter element was tested in the cold-flow filter model, but the collection efficiency did not meet selection requirements.

Filter Element Configuration. For all of the gasification testing conducted in BP2, the PCD was configured with a total of 72 filter elements, which are given in Table 27. Since the PCD was not opened between tests, the same filter element configuration was used for all three test campaigns with a total exposure to syngas of 2,088 hours.

Table 27. Hot Gas Filter Elements Tested During BP2.

Filter Media Type	Material	Supplier/ Brand	Number Installed	Total Syngas Exposure, hours
Sintered Metal Powder	Iron aluminide	Pall/PSS	20	4,050 to 13,540
Fine Sintered Metal Fiber	HR-160	Pall/Dynalloy	17	3583
Coarse Sintered Metal Fiber	HR-160	Pall/Dynalloy	22	2,088 to 5,610
Sintered Metal Powder	High alloy	Mott	3	2088
Sintered Metal Fiber	Coated high alloy	Porvair/Sinterflo	10	2560

Testing allowed continued exposure of the Pall/PSS iron aluminide sintered metal powder elements along with several different types of sintered metal fiber elements supplied by Pall, Mott, and Porvair. The PCD will be opened early in 2011 for detailed inspection, and the elements will be removed for flow testing, cleaning, and corrosion evaluation.

Qualification Testing of New Filter Elements. Cold-flow particulate collection efficiency tests were conducted with a new type of sintered metal fiber filter element that was in an early stage of development. The prototype element failed to achieve acceptable collection efficiency, normally 99.995 percent for a new filter, but the supplier is working on improvements in the filter element design. When an improved prototype is available, another set of collection efficiency measurements will be made to assess the design improvements made by the manufacturer.

Overall, the results from the cold-flow PCD testing continued to show that the collection efficiency of the sintered metal fiber elements increases with decreasing fiber size. However, the finer fiber size also produces a higher pressure drop and is more vulnerable to corrosion. As noted previously, the sintered metal powder elements tend to give higher collection efficiencies than do the sintered metal fiber elements due to the more tortuous flow path through the filter media. Collection efficiencies in excess of 99.9999 percent can be achieved with the sintered metal powder media and with other media that have been conditioned in the PCD.

5.6 JOHNSON MATTHEY MERCURY SORBENT

In collaboration with the NETL, Johnson Matthey has been developing a solid, sorbent-based process to remove mercury and other trace contaminants, such as arsenic and selenium, at high temperature in coal gasification processes. Compared to low-temperature capture by activated carbon, high-temperature capture of these trace elements retains the high thermal efficiency of the coal gasification process in IGCC power plants.

The high-temperature, palladium-based, mercury adsorbent supplied by Johnson Matthey was tested in runs R04 and R05 in the SCU. Around 10 pounds of sorbent (which had been reduced on site to its metallic form) were placed in a pressure vessel in a fixed-bed arrangement. A catalyst bed height of 14 inches was selected to achieve the required space velocity of 2,800/hr. Table 28 lists the test conditions.

Table 28. Operating Conditions for Mercury Sorbent.

	Test Run R04	Test Run R05
Syngas Flow Rate, lb/hr	10	25
Operating Temperature, °F	500	500
Operating Pressure, psia	195	195
Hours of Operation	500	720
Palladium Content, wt%	2	5

The objectives of the test program are to:

- Determine durability of sorbent under commercially realistic operating conditions
- Improve candidate sorbent capacities
- Elucidate mercury-sorbent interactions

During R04, ten gas samples, five each from the inlet and outlet of the sorbent bed, were collected using a modified EPA Method 29 for trace metal analysis of mercury, arsenic, and selenium. Breakthrough of each species occurred between the times the last two samples were taken, but prior to that collection efficiency was near 100 percent. During R05 twelve gas samples, six each from the inlet and outlet of the sorbent bed were collected. No breakthrough of the three species was detected, indicating that the beds were not saturated. The absence of breakthrough during the R05 could be partially explained by the lower inlet mercury concentration. Figure 55 provides syngas mercury concentrations during R04 and R05. After both test runs, the sorbent was removed from the bed in seven layers and returned to the Johnson Matthey company for analysis.

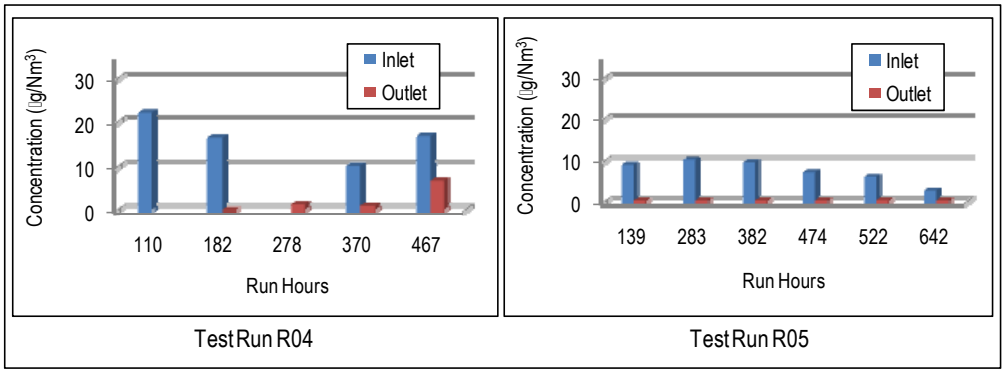

Figure 55. Reactor Inlet and Outlet Mercury Concentrations during Sorbent Testing.

NETL Mass Spectrometry. During R05, a Gas Chromatograph-Inductively Coupled Plasma/Mass Spectrometry (GC-ICP/MS), shown in Figure 56, which is under development at NETL, was

incorporated into the mercury sorbent test. This instrument allows for on-line measurement of trace metal concentrations. To prevent trace metal adsorption in the sample tube delivering syngas to the instrument, the inner surface was coated with one-micron thick silicon oxide barrier layer.

Figure 56. GC-ICP/MS at DOE-NETL Laboratory.

This was first time this instrument was used in the field to measure mercury concentrations directly. Data were collected continuously every 15 minutes. Although measured mercury levels from the GC-ICP/MS were higher than those determined by the EPA method, the results demonstrated the potential to gather real-time data and to facilitate control over key parameters. More analysis is being conducted at NETL to understand the discrepancy. In addition, NETL researchers are incorporating lessons learned during R05, which includes improving the heat tracing of sampling loops and controls for system pressure and syngas flow. The instrument will be tested further during future test runs.

6.0 CONCLUSIONS AND LESSONS LEARNED

Conclusions and lessons learned from studies and from experience gained during BP2 are discussed in the following sections.

6.1 TECHNOLOGY ASSESSMENT

- Both PCC and TROC require a significant capital investment and negatively affect plant performance.
- Both PCC and TROC are capable of recovering a minimum of 90 percent of the CO_2 produced by the plant, and some TROC configurations can capture 99 percent if the CO_2 product purity is decreased
- Both PCC and TROC (in one configuration) are capable of meeting typical industry CO_2 product specifications, including some for enhanced oil recovery
- If high product purity is not required, the TROC capital cost can be reduced by choosing a configuration with less CO_2 purification, while still achieving a purity sufficient for sequestration
- Although the results show 3 to 12 percent lower capital costs for TROC compared with PCC (on a $/kW basis), the difference is within the accuracy of the estimate
- Although a space-constrained site adds to the capital cost of TROC, Case 5 suggests that the increment is not excessive
- TROC has lower heat rates and O&M costs compared with PCC resulting in a 10 to 16 percent lower LCOE, at 75 percent capacity factor, and this advantage widens if dispatch differences are considered
- It is expected that PCC and TROC dispatch rates would be significantly different since the TROC dispatch costs (fuel plus variable O&M) are 24 to 26 percent lower than for PCC

6.2 PRE-COMBUSTION CO_2 CAPTURE AND SEPARATION

- Water-gas shift reaction testing showed that sufficiently high CO conversions were achieved at lower than recommended steam-to-CO ratios and that only marginal increases in conversion would be realized for ratios above 1.6. No methane was formed and no carbon was deposited in the reactor.
- The evaluation studies also indicated that for a 500-MW IGCC plant, a steam-to-CO ratio of 0.1 corresponded to 4 MW of power, so operating with excess steam would have a significant impact upon net power production. For example, if a steam-to-CO ratio of 1.6 was acceptable rather than 2.6, then an additional 40 MW would be available for distribution to the grid.
- Measured concentrations of ammonium carbamate and ABC were predicted with good accuracy by the OLI model and any error associated with ammonium carbonate was low. This was considered to validate the model and allow it to be used with confidence for predicting the composition of the ammonia liquor.
- Testing of ammonia sorbent regeneration showed that despite the temperature increase, no ammonium bicarbonate decomposed, and no CO_2 was released. Results suggested that the liquor re-established chemical equilibrium at the new temperature. At around 60°C, CO_2

release began, but ammonium bicarbonate was being formed and did not start to decompose until the temperature was around 80°C.

- Controlling the sorbent absorption temperature at 40°C requires additional cooling to remove the heat released when the ammonium bicarbonate crystallizes. When regeneration is required, heat must be added to dissolve the crystals and the temperature raised to above 80°C before significant CO_2 is released. Cooling duty and water usage could be reduced if absorption could be carried out effectively closer to 60°C. This would also reduce the sensible heat required (some of which is recovered using recuperators) to raise the liquor to regeneration temperature.
- A possible drawback of operating the absorber at 60°C is an increase in ammonia slip in the exiting CO_2-depleted syngas. The ammonia would be scrubbed out using water wash, although this constitutes a system loss. The feasibility of operating the absorber at temperatures greater than 40°C will be assessed with additional modeling and batch reactor testing.
- Agreement between the data from OLI modeling and from the Raman Spectroscope was not good, and comparisons of ammonium carbamate and carbonate were similarly poor. More testing and analysis is required to understand how to achieve a correlation that is applicable to all concentrations of ammonia. The incentive for resolving this issue is that the Raman probe with its rapid response could potentially be used to monitor and control a commercial process.
- SCU test data showed that with or without water addition, DEPG achieved higher absorption efficiencies than PDMS for initial and subsequent cycles. Also, the CO_2 concentration profile indicated that absorption was maintained for a longer period, allowing DEPG to achieve a higher loading level. From the area within the concentration profiles, the CO_2 loading for DEPG was approximately 1.4 times higher than that for PDMS.
- The H_2S concentration profiles indicated that absorption was maintained for a longer period with DEPG than with PDMS. From the area within the concentration profiles, the H_2S loading for DEPG is approximately 3.5 times higher than that for PDMS.
- The CO_2 mass loading for ammonia was shown to be greatly in excess of potassium carbonate and potassium prolinate, with the potassium carbonate having the lowest loading.
- During testing of the MTR CO_2 membrane, the CO_2 concentration in the permeate was 4 to 5 times that of the feed steam, and the H_2S concentration was about 6 times higher in the permeate than in the feed stream. During the testing, the membrane operated stably with variations occurring primarily from changes in ambient temperature, with a lesser effect of syngas composition and flow rate.
- Results from MTR's hydrogen membrane tests indicated that hydrogen in the feed stream was enriched 6 to 8 times in the permeate stream. The presence of H_2S in the syngas feed did not compromise membrane performance.
- Both the CO_2-selective Polaris membrane and H_2-selective Proteus membrane from MTR performed well using coal-derived syngas. The results were consistent with those from MTR's bench-scale test using simulated syngas. Stable membrane performance under industrial conditions is encouraging for further development of polymeric membrane technology.

- Test results indicate that the MPT carbon molecular sieve membrane operating at 530°F can be used to separate hydrogen from raw syngas without reduction in performance. This temperature is compatible with water gas shift catalytic reactor temperature indicating that the water-gas shift reaction and hydrogen separation could potential be incorporated into a single unit process.
- Coupon testing of potential membrane materials showed that material consisting of only palladium sulfides failed within 1,000 hours of exposure. The resistance to corrosion was increased as the percent of copper in the coupon material increased.

6.3 POST-COMBUSTION CO_2 CAPTURE

- The PC4 site preparation work included recovery of an area from the Plant Gaston coal pile run-off pond, leveling and compaction of the site, and commencement of caisson installation. A total of 75 caissons and 30 micropiles were required to provide a solid base for continued installation of foundations and other civil engineering components. The micropiles were required in some areas where existing underground piping and electrical conduits could not be rerouted. In addition, 54 piers were installed at the top of the caissons in preparation of setting support columns for utility bridge modules.
- The PSTU design included development of a 3-D model, which greatly assisted field personnel during fabrication.
- Quality control procedures were developed, which will be employed to ensure that data collected is of the highest possible value.
- Analytical methods will require further development to be used in the unique applications of the PC4.
- The establishment of the PSTU commissioning and start-up team was key in personnel training, procedure development, and other preparations which all worked to keep the commissioning on schedule.

6.4 GASIFICATION PROCESS

- The increased reliability of level probe indications provided by the vibration-type probes in the PDAC feeder allow the lock vessel filling cycle to be optimized by using the level probe indication to end the fill cycle instead of waiting for the timer to time out. The benefit of this change is especially significant when operating the feeder at higher feed rates.
- Optimization of the PDAC instantaneous feed rate feedback control resulted in decreased feed rate variability as indicated by the conveying line differential pressure indication.
- Controlling the PDAC feeder silo at a higher level promoted a mass flow regime from the bin, decreasing material segregation that can lead to coal feed rate fluctuations.
- Operation of the gasifier with biomass/coal blends yielded steady state carbon conversions averaging over 99 percent. During operation with biomass, the gasification process operated with reliable feeding and with no evidence of ash agglomeration, corrosion, or excessive tar formation.
- Because of the low ash content of the biomass, the addition of biomass reduced the inlet ash concentration with both the PRB coal and the Mississippi lignite. The addition also increased the bulk density and true density of the ash, while reducing the bulk porosity and

surface area. The loss on ignition was also reduced, suggesting that the biomass addition improved carbon conversion.

- For both PRB and Mississippi lignite coals, the gasification ashes produced with biomass co-feeding had lower drag than the ashes produced by coal feeding alone.
- Based on ash characterization studies, the addition of biomass would not have an adverse effect on PCD pressure drop.
- The performance of the sapphire thermowell in the gasifier riser degraded slightly. Additional insight into the observed performance will be pursued with representatives of Emerson Process Management, who supplied the thermowell, pending the outcome of the transmitter investigation.
- Operation of the flow meter during R04 with Mississippi lignite showed good agreement when compared to the existing weigh cell loss of weight calculation. The measurement was also sensitive to instantaneous changes in coal feed rate when compared to existing conveying line differential pressure readings. During R05, the flow meter again displayed good agreement with the weigh cell calculation at higher flow rates. However, during low feed rates with PRB coal during R05, the agreement was poor. The meter will be recalibrated for future service to improve performance.
- After R05, the Dynatrol level probes had operated for over 2,500 hours providing consistent indication of solids levels inside the vessels for both lignite and subbituminous coals.
- A Drexelbrook point sensitive level probe, installed to maintain a higher level control in the PCAD lock vessel, operated reliably after re-calibration.
- Test data indicated that gasifier solids circulation rate could be controlled to low levels by varying only the fluidization to the bottom of the standpipe.
- A new gasifier temperature control scheme demonstrated good control of gasifier mixing zone temperatures using standard proportional–integral–derivative controllers to adjust air flow to the different zones while maintaining a constant total air flow to the gasifier. Since gasifier upper and lower mixing zone temperatures respond rapidly to changes in air feed rate, the temperature controllers were tuned to respond slowly to minimize temperature overshoot.
- At the end of BP2 testing, the gasification process had operated for almost 15,000 hours on coal.
- During the gasification test runs, the PCD operation with very high collection efficiency (>99.999%) and without any filter element failures. The elements used included various metal elements supplied by Pall, Mott, and Porvair. Some of the elements have been exposed to gasification operation for over 13,500 hours.
- Results from cold-flow PCD testing continued to show that the collection efficiency of the sintered metal fiber elements increases with decreasing fiber size. However, the finer fiber size also produces a higher pressure drop and is more vulnerable to corrosion.
- In hot gas filter operation, collection efficiencies in excess of 99.9999 percent can be achieved with the sintered metal powder media and with other media that have been conditioned from previous operation.
- Testing of the Johnson Matthey palladium-based mercury sorbent indicated collection efficiencies near 100 percent.

- Although measured mercury levels from NETL's GC-ICP/MS were higher than those determined by the EPA method, the results demonstrated the potential to gather real-time data and so facilitate control over key parameters. NETL researchers are incorporating lessons learned during R05, which includes improving the heat tracing of sampling loops and controls for system pressure and syngas flow.